A Benchmark Database for Mixed-Solvent Electrolyte Solutions: Consistency Analysis using E-NRTL

Fufang Yang, Tri Dat Ngo, Georgios Kontogeorgis, Jean-Charles de Hemptinne

A benchmark database for mixed-solvent electrolyte solutions: Consistency analysis using E-NRTL

Fufang Yang [1,2], Tri Dat Ngo [1], Georgios M. Kontogeorgis [2], Jean-Charles de Hemptinne [1]*

[1] IFP Energies Nouvelles, 1 et 4 Avenue de Bois-Préau, 92852 Rueil-Malmaison Cedex, France

[2] Center for Energy Resources Engineering (CERE), Department of Chemical and Biochemical Engineering, Technical University of Denmark, 2800 Kgs. Lyngby, Denmark

* Corresponding author: jean-charles.de-hemptinne@ifpen.fr

Abstract: Modeling of thermodynamic properties of mixed-solvent electrolyte solutions is challenging. Reliable experimental data are essential for any model development and parameterization. In this work, a benchmark database for (water + methanol/ethanol + alkali halide) mixed-solvent electrolyte solutions is presented. Available experimental data of mean ionic activity coefficient (MIAC) and vapor-liquid equilibrium (VLE) are comprehensively collected and critically evaluated for 61 datasets of 23 solutions. The resulting benchmark database includes 1413 data records from 32 datasets for 13 solutions. Evaluated datasets of the relevant aqueous electrolyte solutions are also presented. A consistent E-NRTL model that satisfies the Gibbs-Duhem equation is utilized for analyzing the data, reconciling the MIAC and VLE data. The collected data are critically evaluated. A benchmark database is obtained. Based on the database, recommended parameters are obtained for the E-NRTL model.

Keywords: benchmark database, consistent E-NRTL, mixed-solvent electrolyte solution, mean ionic activity coefficient, vapor-liquid equilibrium

1 Introduction

Electrolyte solutions are important in many industrial processes, e.g., CO_2 capture and sequestration [1], flue gas treatment [2], desalination [3], scale formation [4], corrosion resistance enhancement [5], batteries [6], pharmaceutical processes [7], etc. Reliable experimental data are essential for thermodynamic property model development and process system modeling, while incomplete

and inaccurate data hampers their utilization [8]. Because of the complexity of the interactions that take place in electrolyte solutions, the existing thermodynamic models are not well adapted to those mixtures [9]; available tools are not yet well accepted and validated as for non-electrolyte systems [10]; the physics of the competing contributions is not yet well understood [11,12]. Furthermore, over the past century, experimental data have been reported in dozens of conventions [13], e.g., different reference states and composition units. In addition, for mixed-solvent electrolyte solutions, experimental data from different sources are frequently not consistent with each other. Thus, obtaining a reliable database needs comprehensive collection and critical evaluation of available experimental data.

In a previous work [14], a benchmark database is proposed for aqueous alkali halide solutions. For mixed-solvent electrolyte solutions, the extra solvent brings in an extra dimension in composition, complexing property comparisons. Furthermore, the solvation and dissociation behavior of electrolytes is very different in water and non-water solvents. Various equations of state [15–25] and activity coefficient models [26–38] have been applied on these mixtures. Because of the complexity from both experimental and theoretical perspectives, a benchmark database for important mixtures of the type can facilitate future model development, parameterization, and evaluation. In addition, compared to the data status of aqueous electrolyte solutions, that of mixed-solvent electrolyte solutions is much scarcer. Therefore, data analysis requires a model that applies on mixed-solvent electrolyte systems and does not include too many adjustable parameters.

Although modern thermodynamic models are of theoretical basis. As parameters are regressed, accurate correlation of the experimental data does not guarantee data reliability. Therefore, critical evaluation of the experimental data needs comparisons between data from different sources and of different properties, as well as comparisons within a series of salts in the same solvents. To achieve this, a consistent version of the E-NRTL model is introduced, satisfying the Gibbs-Duhem equation, and thus facilitating verification between the mean ionic activity coefficient (MIAC) and vapor-liquid equilibrium (VLE), which includes information of the ionic and solvent activity coefficients, respectively. The consistent model is similar to the consistent model proposed by van Bochove et al. [31], short of the Bronsted-Guggenheim term [39,40].

Our aim is to present a benchmark database based on an extensive evaluation of available experimental data, to recommend parameters based on this database, and to understand trends of

data and parameters. The work proceeds as follows. First, the overall data analysis framework is introduced. Then, the consistent E-NRTL model is introduced and compared with the widely used original E-NRTL. Then, a consistency analysis is performed for each mixture. Impacts of the objective function and water-salt parameters on the representation of mixed-solvent electrolyte solution properties are investigated, concluding on a parameter regression procedure that facilitates the data analysis framework. Based on these findings, the alcohol-salt parameters and ternary property results are presented. Finally, the obtained benchmark database of the mixed-solvent electrolyte systems and the involved aqueous electrolyte systems is proposed.

2 Data analysis framework

This section introduces the properties' definitions and relationships with the activity coefficients, the composition denotations, and the raw data collected from the databanks. Figure 1 shows the data analysis framework. The following path is followed:

(1) We start from the raw data collected from the databanks. Datasets that are non-experimental and incomplete (e.g., datasets that are not in tabular forms, and VLE datasets without vapor phase molar fraction) are removed. The experimental datasets were reported in many different composition units. They are converted to ion-based molar fraction, i.e., full dissociation is assumed, and the cation and anion are considered as two species. For the (water + alcohol) mixtures, VLE data are collected. For the (water + salt) and (water + alcohol + salt) mixtures, VLE and MIAC data are collected. For mixtures containing two solvents, only the VLE datasets that include both vapor pressure and vapor phase molar fraction data are collected, because solvent activity coefficient requires both variables.

(2) Then, the binary datasets are compared against each other and with the E-NRTL model with preliminary parameters. Doing so, inconsistent datasets are spotted as they do not agree with data from multiple other sources (for binary mixtures, the data status is quite extensive, and there are always datasets from multiple sources that agree with each other), and are removed. The remaining datasets constitute the benchmark database of the binary mixtures.

(3) Based on these datasets, parameters are regressed for the water-alcohol and water-salt pairs. Once these parameters (water-alcohol and water-salt) are sufficiently validated, they are used in the evaluation of the ternary (water + alcohol + salt) datasets, along with preliminary parameters for the alcohol-salt pairs. Because the solubility of salts in anhydrous alcohol is

usually very small, in which range the model is dominated by the Pitzer-Debye-Huckel (PDH) term, regression of the parameters of the alcohol-salt pairs to binary (alcohol + salt) data is infeasible. Mixed-solvent electrolyte solution data are more suitable for obtaining alcohol-salt parameters. Therefore, the binary (alcohol + salt) mixtures are not included in this benchmark database. Compared to the data status of the aqueous electrolyte solutions, that of the mixed-solvent electrolyte solutions is not as extensive. The datasets are evaluated by comparing with other datasets for the same mixture when they are available, and by observing the data trends to identify obvious outliers. Inconsistent datasets are identified and removed. The remaining datasets are further marked as “recommended”, “tentative”, and “uncertain”, constituting the benchmark database of the mixed-solvent electrolyte solutions. Based on the database, parameters of the E-NRTL model are regressed.

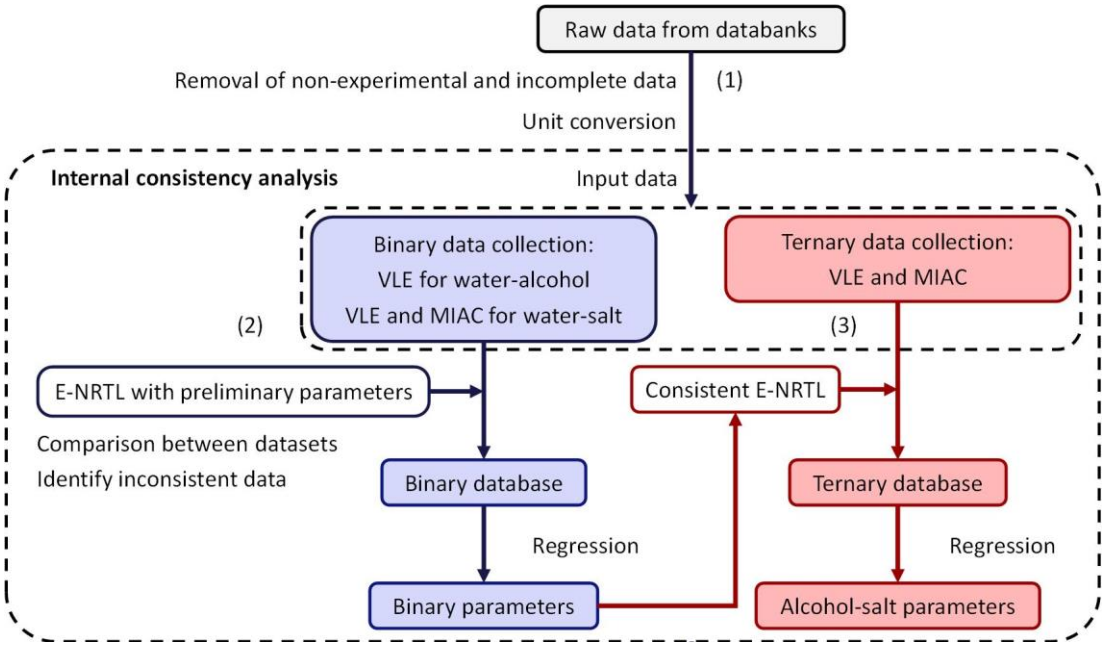

Figure 1. Data analysis framework.

2.1 Properties and their relationships with the activity coefficients

MIAC and VLE include information about the derivatives of the excess Gibbs energy (G^E) with respect to salt and solvent molar fractions, as shown in Figure 2. The arrow direction denotes that the composition derivatives of G^E are for the corresponding components. By definition, MIAC relates to the derivative of G^E over the salt composition, while VLE relates to the derivative of G^E over the solvent compositions. Therefore, they are ideal for model parameterization, and are included in the database.

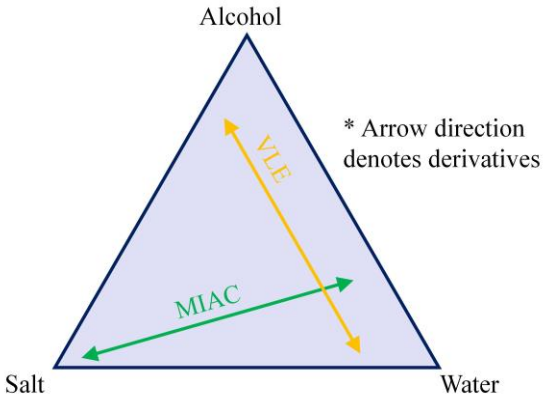

Figure 2. Schematics of the correspondence between the properties and composition derivatives of G^E.

The activity coefficient describes deviation from ideality based on a given reference state and composition unit. For ions, a common convention of the activity coefficient is the rational asymmetrical activity coefficient. For aqueous electrolyte solutions, the ionic activity coefficient is normalized at infinite dilution in the water solvent. For mixed-solvent electrolyte solutions, the ionic activity coefficient is normalized at infinite dilution in the solvent mixture at the same salt-free composition, because, otherwise, large experimental composition uncertainties would be present at low water composition when properties are defined in the molality unit. In the experimental literature, data are always reported based on the molality unit defined in the solvent mixture.

$$\gamma_i^* = \frac{\gamma_i}{\gamma_i^\infty} \tag{1}$$

where γ_i is the symmetrical activity coefficient, γ_i^∞ is γ_i at infinite dilution in the solvent mixture at the corresponding salt-free composition. Thus, the reference state in Eq. (1) is different according to the salt-free composition of the solvent mixture. However, the rational asymmetrical activity coefficient, as well as the molality and molarity conventions, are only used for presentation; while γ_i itself is calculated in the models. In this work, unless otherwise noted, the reference state of ionic activity coefficient is defined at infinite dilution in the solvent mixture.

In addition, the molality activity coefficient (γ_i^{m}) and molarity activity coefficient (γ_i^{c}) are also widely used conventions:

$$\gamma_i^{\mathrm{m}} = \gamma_i^* \sum_j^{\text{solvents}} x_j \tag{2}$$

$$\gamma_i^{\mathrm{c}} = \gamma_i^* \frac{\rho_{\mathrm{solvent}}}{\rho_{\mathrm{solution}}} \tag{3}$$

where ρ is the mass density. Like γ_i^*, γ_i^{m} and γ_i^{c} also take reference state at infinite dilution in the solvent mixture at the corresponding salt-free composition.

The MIAC is usually reported in the experimental literature in the molality convention.

$$\gamma_{\pm}{}^{\mathrm{m}} = ({\gamma_{\mathrm{c}}}^{\mathrm{m}\nu_{\mathrm{c}}} {\gamma_{\mathrm{a}}}^{\mathrm{m}\nu_{\mathrm{a}}})^{\frac{1}{\nu}} \tag{4}$$

where $\nu = \nu_{\mathrm{c}} + \nu_{\mathrm{a}}$ is the sum of the stoichiometric coefficients, the subscript c denotes cations, and the subscript a denotes anions.

The MIAC is usually measured using potentiometry (also noted as electromotive force measurement) [41]. An alternative approach is to calculate MIAC based on the Gibbs-Duhem equation, e.g., the isopiestic vapor pressure measurements conducted by Robinson and co-workers for many aqueous solutions [42–44]. However, for mixed-solvent electrolyte solutions, an infinite dilution activity coefficient model is needed for converting the reference state of these data to the infinite dilution of the salt in the solvent mixture at the same salt-free solvent composition. In this work, all the collected data are measured by potentiometry. This reflects what has been unanimously implemented in the experimental community. In the potentiometric measurements, the electromotive force of the cells are measured, and substituted into the Nernst equation as a function of molality (defined in the solvent mixture) along with an activity coefficient model, e.g., the extended Debye-Hückel. With some treatment, the expression is close to linear with molality [13,45]. Coefficients of the Nernst equation and the activity coefficient model are regressed at the same time for each salt-free composition. The obtained coefficients are then used for calculating the MIAC. Thus, the reported MIAC depends not only on the measurement of the particular salt molality, but also on the series of measurements for the salt-free solvent composition.

In the experimental literature, the uncertainty of electromotive force measurement, rather than of the MIAC itself, is usually reported. The electromotive force can be measured up to very high accuracy, e.g., 0.02 mV, corresponding to 0.05% in the MIAC [41]. However, the abovementioned data treatment procedure introduces uncertainty in the obtained MIAC. Furthermore, the measurement uncertainties of composition and temperature also contribute to the combined uncertainty of the MIAC.For mixed-solvent electrolyte solutions, the relatively large deviations (in

some cases more than 20%) observed in mixed-solvent electrolyte measurements from different experimental sources is a matter of reliability rather than accuracy, indicating an imperative need for critically evaluating the data before use in model developments.

When the mixed-solvent electrolyte solution VLE data include both vapor pressure and vapor phase molar fraction, the solvent activity coefficient can be obtained taking the ideal gas assumption in the vapor phase,

$$\gamma_{i,\text{solvent}} = \frac{y_{i,\text{solvent}} p}{x_{i,\text{solvent}} p^{\text{sat}}_{i,\text{solvent}}} \tag{5}$$

where y is the molar fraction in the vapor phase, x is the molar fraction in the liquid phase, p is the pressure, $p^{\text{sat}}_{i,\text{solvent}}$ is the vapor pressure of pure solvent i at the temperature. Eq. (5) assumes that the pressure is sufficiently small so that the vapor phase can be treated as ideal gas and that no Poynting correction is needed in the liquid phase. Figure 3 shows the solvent activity coefficients derived from experimental VLE data for (water + ethanol + KCl) at 298.15 K using Eq. (5). As salt composition increases, alcohol activity coefficient increases, while water activity coefficient decreases. The alcohol activity coefficient changes more with the salt composition at low alcohol composition, while the water activity coefficient is close to unity in the entire experimental data range. As alcohol composition increases, alcohol activity coefficient decreases, while water activity coefficient first decreases and then increases.

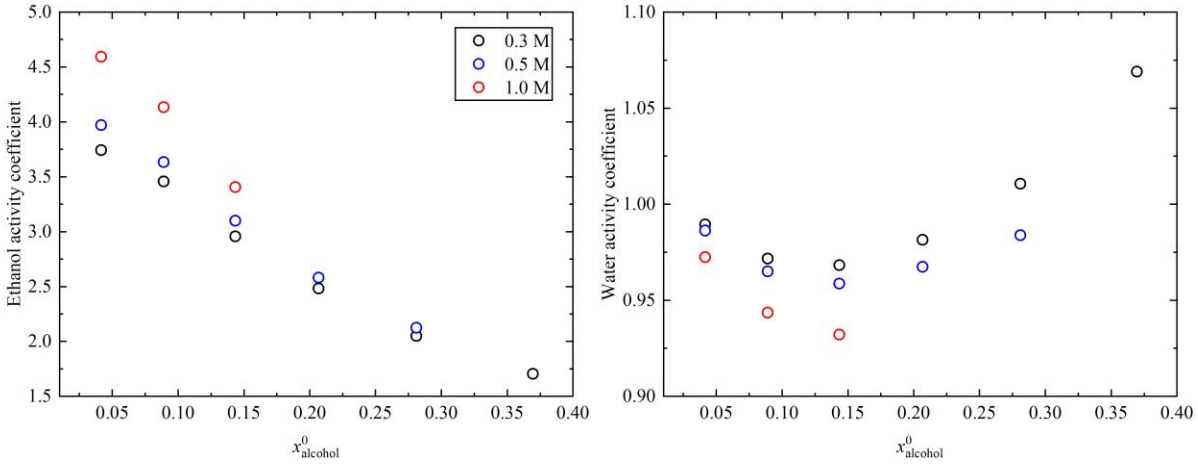

Figure 3. Solvent activity coefficients derived from experimental VLE data [46] for (water + ethanol + KCl) at 298.15 K.

The ionic and solvent activity coefficients are related to each other according to the Gibbs-Duhem equation. At constant T and p,

$$\sum n_{i,\mathrm{solv}} \mathrm{d}\ln x_{i,\mathrm{solv}}\gamma_{i,\mathrm{solv}} + n_s \sum \nu \mathrm{d}\ln m_{\pm}\gamma_{\pm}^{m} = 0 \quad (6)$$

Therefore, MIAC and VLE are complementary to each other. Experimental data of these properties can be utilized to verify each other.

2.2 Composition denotations

Experimental data were reported in many different conventions. Typically, for mixed-solvent electrolyte mixtures, solvent compositions were usually reported in molar fraction or weight fraction on the salt-free basis, while salt compositions were usually reported in molar fraction, molality, or molarity. Before any modeling work, these data need to be converted to the same unit, typically ion-based molar fraction, which is used in most models. For instance, the composition unit of salt-free molar fraction for solvent and molality for salt can be converted to ion-based molar fraction according to,

$$x_{i,\mathrm{solvent}} = \frac{1000\ \mathrm{g} \times \sum_j \frac{x^0_{j,\mathrm{solvent}}}{M_{j,\mathrm{solvent}}}}{\nu x^0_{\mathrm{salt}} + 1000\ \mathrm{g} \times \sum_j \frac{x^0_{j,\mathrm{solvent}}}{M_{j,\mathrm{solvent}}}} \quad (7)$$

$$x_{i,\mathrm{ion}} = \frac{\nu_i x^0_{\mathrm{salt}}}{\nu x^0_{\mathrm{salt}} + 1000\ \mathrm{g} \times \sum_j \frac{x^0_{j,\mathrm{solvent}}}{M_{j,\mathrm{solvent}}}} \quad (8)$$

where x^0 is in the original composition unit before conversion, M is the molar mass, and the subscript ion denotes cation or anion. In this work, we consider only the alkali halides. Hence, $\nu = 2$, $\nu_i = 1$.

2.3 Raw data collected from databanks

Data are collected from DETHERM [47], CERE electrolyte databank [48], and other sources, e.g., datasets that were utilized in other modeling papers (e.g., references [16,19,21,23–25]), etc. All the collected data are experimental and available in public literature. Datasets that are not provided in tabular forms are excluded. VLE datasets that do not report both vapor pressure and vapor phase molar fraction are excluded. Among those mixtures, experimental data are more extensive for the mixtures containing Na^+ salts and Cl^- salts. Overall, the data status of the mixed-solvent electrolyte mixtures is much less extensive compared to that of aqueous alkali halide mixtures [14]. Data of the

constituting (alcohol + salt) binary mixtures are not included in the database, because the data status is even scarcer compared to that of the mixed-solvent electrolyte solutions, because that MIAC data is almost nonexistent, and because salt solubility is very small in alcohols in most cases.

After collecting the raw database and evaluating the data quality, a final database is constructed by introducing some codes ("**R**" for "recommended", "**T**" for "tentative", and "**U**" for "uncertain"). Details will be explained in Section 6.

2.4 Statistical quantities' definitions

In what follows, the data will be compared with calculation results, resulting in the need for defining some statistical quantities.

Average deviation (AD) and maximum deviation (MD): AD and MD represent deviations of the model from each experimental dataset. For vapor pressure, the relative deviation is taken. For vapor phase molar fraction and MIAC, the absolute deviation is taken. The vapor phase molar fraction is between 0 and 1, while MIAC is in general between 0 and 1 in the salt composition range that is used in the parameter optimization in this work. Using the absolute deviation rather than the relative deviation avoids exaggerating the deviations when the values are small. In the data analysis, x_{ion} is limited to 0.06, in which range MIAC is never much larger than 1. However, if MIAC gets very large in the regression data, relative deviation should be used.

Objective function (OF): Parameters are optimized using a local minimizer in IFPEN's optimization software, ATOUT [49], starting from the optimal value from 50 initial parameter sets randomly obtained in the parameter ranges using a Latin hypercube algorithm. The combined objective function (OF) is,

$$\mathrm{OF} = \frac{1}{2}\sum_{j=1}^{n_{\mathrm{ds}}} \frac{\sum_{i=1}^{n_{\mathrm{dp}}^{j}} \left(\gamma^{\pm}{}_{\mathrm{cal}}^{\,i,j} - \gamma^{\pm}{}_{\mathrm{exp}}^{\,i,j}\right)^2}{n_{\mathrm{dp}}^{j}} + \frac{1}{2}\sum_{j=1}^{n_{\mathrm{ds}}} \frac{\sum_{i=1}^{n_{\mathrm{dp}}^{j}} \left(\frac{p_{\mathrm{cal}}^{i,j} - p_{\mathrm{exp}}^{i,j}}{p_{\mathrm{exp}}^{i,j}}\right)^2}{n_{\mathrm{dp}}^{j}} + \frac{1}{2}\sum_{j=1}^{n_{\mathrm{ds}}} \frac{\sum_{i=1}^{n_{\mathrm{dp}}^{j}} \left(y_{\mathrm{cosolvent,cal}}^{i,j} - y_{\mathrm{cosolvent,exp}}^{i,j}\right)^2}{n_{\mathrm{dp}}^{j}} \tag{9}$$

where n_{ds} is the number of datasets, n_{dp}^{j} is the number of data points in dataset *j*, the subscript cal denotes calculated values, and the subscript exp denotes experimental values. Depending on the data status, MIAC and VLE are used individually or together for the different mixtures. In the following sections, the OF that only consists of MIAC data is denoted as OF-M, the OF that only consists of VLE data (pressure and vapor phase molar fraction) is denoted as OF-V, and the OF that consists of both MIAC and VLE is denoted as OF-MV. Quite often, uncertainty is not reported in the experimental literature. In addition, the uncertainty might be reported more optimistically in some experimental literature than others. Instead of using directly the data uncertainty as reported, a more rigorous approach is to adjust its value based on data distribution, observed deviation after correcting systematic deviations, and model capability [50]. However, the availability of experimental data and uncertainty of the mixed-solvent electrolyte solutions does not facilitate such detailed analysis. Therefore, the data uncertainty is not included in the data analysis. Instead, the same weight is assigned to all the datasets that are considered to be reliable after extensive comparisons between datasets from different experimental sources.

3 Model for data analysis

The electrolyte non-random two-liquid (E-NRTL) model [51,52] is used for data analysis because of its wide acceptance in the industry [53], its capacity to describe mixed-solvent electrolyte solutions [27], its small number of adjustable parameters, and its potential theoretical basis of parameters [54]. The E-NRTL model includes a NRTL part [55], which accounts for the local interaction contribution between all interacting species, and a PDH part [56], which accounts for the long-range Coulombic interaction contribution between ions. Mock et al. [26] applied the E-NRTL model on mixed-solvent electrolyte mixtures, which was implemented in ASPEN PLUS. However, according to these authors, "only the local interaction contribution term of the electrolyte NRTL model is used in this study and the long-range interaction contribution term is dropped", because their "main consideration was the ability to represent the phase equilibrium behavior of solvent species". The model was successful in representing VLE. Liu and Watanasiri [57] introduced a Bronsted-Guggenheim term [39,40] and a Born term [58,59] into the model, and applied the E-NRTL model on the representation of liquid-liquid equilibrium of mixed-solvent electrolyte solutions. Van Bochove et al. [31] suggested that the difference in the dielectric constants of the solvents were large in the (water + organic solvent + salt) mixtures, and included the correct solvent composition derivatives in their

PDH and Born terms. The resulting E-NRTL model satisfies the Gibbs-Duhem equation, and thus is consistent. However, they suggested that the consistent e-NRTL is only slightly better than original e-NRTL. In a recent work, Chang and Lin [60] included the ion contribution to the solvent-related properties in their extended PDH model. However, van Bochove's derivations were largely ignored in later works on mixed-solvent electrolyte modeling with the E-NRTL model. The Born term [58,59] in the E-NRTL model accounts for the difference of medium effect between the infinite-dilution aqueous solution to the given mixed-solvent solution. Song and Chen [27] proposed a segmental E-NRTL model for mixed-solvent electrolyte solutions, and later proposed a symmetrical version [61] to accommodate pure fused salts. In these works, the solvent density and relative permittivity were considered as pseudo-pure functions, i.e., although solvent-composition dependence was accounted for in the function, derivative terms were omitted as activity coefficients were derived from the excess Gibbs energy. Tsanas et al. [62] suggested that violation of the Gibbs-Duhem equation would result in convergence to the wrong minimum in reactive flash calculations. In this section, the consistent E-NRTL model is described; then, the consistent and original E-NRTL models are compared to show whether the issue of consistency matters for VLE and MIAC calculations, which are the scope of the presented database in this work.

3.1 Consistent E-NRTL

For mixed-solvent electrolyte solutions, the original E-NRTL [27,61] is usually used in a manner that violates the Gibbs-Duhem equation. (The problem is not present for single-solvent systems.) In Van Bochove et al.'s work [31], the model satisfies the Gibbs-Duhem equation, and therefore is consistent. In the consistent E-NRTL model, the PDH and Born terms are different from the original E-NRTL, as the correct solvent composition derivatives are included. This work utilizes a model that is similar to Van Bochove's consistent model, short of the Bronsted-Guggenheim term. The model consists of a NRTL term, a PDH term, and a Born term. Here, the model is briefly introduced.

The activity coefficient terms are obtained by taking partial derivatives of the excess Gibbs energy terms:

$$\frac{G^{\mathrm{E,PDH}}}{RT} = -\left(\sum_i n_i\right)\frac{4A_\varphi I_x}{\rho}\ln\left(1+\rho {I_x}^{\frac{1}{2}}\right) \tag{10}$$

$$\frac{G^{\mathrm{E,Born}}}{RT} = \frac{{Q_\mathrm{e}}^2}{2kT}\left(\frac{1}{\varepsilon_\mathrm{s}\varepsilon_0} - \frac{1}{\varepsilon_\mathrm{w}\varepsilon_0}\right)\sum \frac{n_i {Z_i}^2}{r_i} \tag{11}$$

where $R = 8.3144598$ J mol^{-1} K^{-1} is the universal gas constant [63], T is the temperature, n_i is the molar number of component i, A_φ is one third of the Debye-Huckel limiting slope as given in Eq. (12), I_x is the ionic strength as given in Eq. (13), $Q_\mathrm{e} = 1.6021766208 \times 10^{-19}$ C is the elementary charge [63], $k = 1.38064852 \times 10^{23}$ m^2 kg s^{-2} K^{-1} is the Boltzmann constant [63], ε_s is the solvent relative permittivity, ε_w is the water relative permittivity, $\varepsilon_0 = 8.854187817 \times 10^{-12}$ F m^{-1} is the dielectric constant in the vacuum [63], Z_i is the ionic charge, r_i is the Born radius and is set at 3 Å for all the ions in this work.

$$A_\varphi = \frac{1}{3}\left(\frac{2\pi N_\mathrm{A}\rho_\mathrm{s}}{1000}\right)^{\frac{1}{2}}\left(\frac{25{Q_\mathrm{e}}^2}{\pi\varepsilon_s\varepsilon_0 kT}\right)^{\frac{3}{2}} \tag{12}$$

$$I_x = {\sum {Z_i}^2 n_i}\Big/{2\sum n_i} \tag{13}$$

where $N_\mathrm{A} = 6.022140857 \times 10^{23}$ mol^{-1} is the Avogadro number [63].

The mixing rules for solvent density and relative permittivity are,

$$\rho_\mathrm{s} = \frac{1}{\sum_i^{\mathrm{solvents}} \frac{x_i^0}{\rho_i}} \tag{14}$$

$$\varepsilon_\mathrm{s} = \sum_i^{\mathrm{solvents}} w_i^0 \varepsilon_i \tag{15}$$

where x_i^0 is the molar fraction on the salt-free basis, w_i^0 is the weight fraction on the salt-free basis, ρ_i is the density of solvent i, and ε_i is the relative permittivity of solvent i, as given below.

$$\rho_i = \frac{A_i}{{B_i}^{1+\left(1-\frac{T}{C_i}\right)^{D_i}}} \tag{16}$$

$$\varepsilon_i = \varepsilon_i^0 + \varepsilon_i^1\left(\frac{1}{T} - \frac{1}{273.15\ \mathrm{K}}\right) \tag{17}$$

The coefficients, A_i, B_i, C_i, D_i, ε_i^0 and ε_i^1, are obtained from or regressed to data from DIPPR [64] and reference [65], as explained in detail in the Supporting Information.

Thus, the activity coefficient terms are,

$$\ln \gamma_i^{\mathrm{PDH}} = \left[\frac{\partial\left(\frac{G^{\mathrm{E,PDH}}}{RT}\right)}{\partial n_i}\right]_{T,p,n_{j(j\neq i)}}$$

$$= \frac{G^{E,\mathrm{PDH}}}{RT}\left\{\frac{1}{\sum_k n_k} + \frac{1}{A_\varphi}\left(\frac{\partial A_\varphi}{\partial n_i}\right)_{T,p,n_{j(j\neq i)}}\right. \tag{18}$$

$$\left. + \frac{1}{I_x}\left(\frac{\partial I_x}{\partial n_i}\right)_{T,p,n_{j(j\neq i)}}\left[1 + \frac{1}{2\left(1+\rho^{-1}{I_x}^{-\frac{1}{2}}\right)\ln\left(1+\rho {I_x}^{\frac{1}{2}}\right)}\right]\right\}$$

$$\ln \gamma_i^{\mathrm{Born}} = \left[\frac{\partial\left(\frac{G^{\mathrm{E,Born}}}{RT}\right)}{\partial n_i}\right]_{T,p,n_{j(j\neq i)}}$$

$$= \begin{cases} -\dfrac{{Q_e}^2}{2kT{\varepsilon_s}^2\varepsilon_0}\left(\dfrac{\partial \varepsilon_s}{\partial n_i}\right)_{T,p,n_{j(j\neq i)}}\left(\sum \dfrac{n_k {Z_k}^2}{100 r_k}\right) & \text{for solvents} \\ \dfrac{{Q_e}^2}{2kT}\left(\dfrac{1}{\varepsilon_s\varepsilon_0} - \dfrac{1}{\varepsilon_w\varepsilon_0}\right)\dfrac{{Z_i}^2}{100 r_i} & \text{for ions} \end{cases} \tag{19}$$

where the analytical expressions for $\left(\frac{\partial A_\varphi}{\partial n_i}\right)_{T,p,n_{j(j\neq i)}}$ and the other derivatives over n_i are provided in the Supporting Information.

The 2nd term in Eq. (18) and the upper equation in Eq. (19) are not included in the original E-NRTL, as derivatives of solvent density and relative permittivity over solvent composition are ignored. As these terms are included, the Gibbs-Duhem equation, which is violated by the original E-NRTL, is satisfied. Consequently, in principle, one can expect that the consistent E-NRTL can reconcile the ion and solvent properties (MIAC and VLE) better.

The consistent E-NRTL model uses exactly the same formulation for the NRTL term as the original E-NRTL [51,52].

$$\ln \gamma_{\mathrm{m}}{}^{\mathrm{NRTL}} = \frac{\sum_j x_j G_{j\mathrm{m}} \tau_{j\mathrm{m}}}{\sum_j x_j G_{j\mathrm{m}}} + \sum_{\mathrm{m}'} \frac{x_{\mathrm{m}'} G_{\mathrm{mm}'}}{\sum_k x_k G_{k\mathrm{m}'}} \left(\tau_{\mathrm{mm}'} - \frac{\sum_k x_k G_{k\mathrm{m}'} \tau_{k\mathrm{m}'}}{\sum_k x_k G_{k\mathrm{m}'}} \right) + \sum_{\mathrm{c}} \frac{\sum_{\mathrm{a}'} \frac{x_{\mathrm{a}'} x_{\mathrm{c}} G_{\mathrm{mc,a'c}}}{\sum_k x_k G_{k\mathrm{c,a'c}}} \left(\tau_{\mathrm{mc,a'c}} - \frac{\sum_{k \neq \mathrm{c}} x_k G_{k\mathrm{c,a'c}} \tau_{k\mathrm{c,a'c}}}{\sum_{k \neq \mathrm{c}} x_k G_{k\mathrm{c,a'c}}} \right)}{\sum_{\mathrm{a}''} x_{\mathrm{a}''}} + \sum_{\mathrm{a}} \frac{\sum_{\mathrm{c}'} \frac{x_{\mathrm{c}'} x_{\mathrm{a}} G_{\mathrm{ma,c'a}}}{\sum_k x_k G_{k\mathrm{a,c'a}}} \left(\tau_{\mathrm{ma,c'a}} - \frac{\sum_{k \neq \mathrm{a}} x_k G_{k\mathrm{a,c'a}} \tau_{k\mathrm{a,c'a}}}{\sum_{k \neq \mathrm{a}} x_k G_{k\mathrm{a,c'a}}} \right)}{\sum_{\mathrm{c}''} x_{\mathrm{c}''}} \tag{20}$$

$$\frac{\ln \gamma_{\mathrm{c}}{}^{\mathrm{NRTL}}}{Z_{\mathrm{c}}} = \frac{\sum_{\mathrm{a}'} \frac{x_{\mathrm{a}'} \sum_k x_k G_{k\mathrm{c,a'c}} \tau_{k\mathrm{c,a'c}}}{\sum_k x_k G_{k\mathrm{c,a'c}}}}{\sum_{\mathrm{a}''} x_{\mathrm{a}''}} + \sum_m \frac{x_{\mathrm{m}} G_{\mathrm{cm}}}{\sum_k x_k G_{k\mathrm{m}}} \left(\tau_{\mathrm{cm}} - \frac{\sum_k x_k G_{k\mathrm{m}} \tau_{k\mathrm{m}}}{\sum_k x_k G_{k\mathrm{m}}} \right) + \sum_{\mathrm{a}} \frac{\sum_{\mathrm{c}'} \frac{x_{\mathrm{c}'} x_{\mathrm{a}} G_{\mathrm{ca,c'a}}}{\sum_k x_k G_{k\mathrm{a,c'a}}} \left(\tau_{\mathrm{ca,c'a}} - \frac{\sum_{k \neq \mathrm{a}} x_k G_{k\mathrm{a,c'a}} \tau_{k\mathrm{a,c'a}}}{\sum_{k \neq \mathrm{a}} x_k G_{k\mathrm{a,c'a}}} \right)}{\sum_{\mathrm{c}''} x_{\mathrm{c}''}} \tag{21}$$

$$\frac{\ln \gamma_{\mathrm{a}}{}^{\mathrm{NRTL}}}{Z_{\mathrm{a}}} = \frac{\sum_{\mathrm{c}'} \frac{x_{\mathrm{c}'} \sum_k x_k G_{k\mathrm{a,c'a}} \tau_{k\mathrm{a,c'a}}}{\sum_k x_k G_{k\mathrm{a,c'a}}}}{\sum_{\mathrm{c}''} x_{\mathrm{c}''}} + \sum_m \frac{x_{\mathrm{m}} G_{\mathrm{am}}}{\sum_k x_k G_{k\mathrm{m}}} \left(\tau_{\mathrm{am}} - \frac{\sum_k x_k G_{k\mathrm{m}} \tau_{k\mathrm{m}}}{\sum_k x_k G_{k\mathrm{m}}} \right) + \sum_{\mathrm{c}} \frac{\sum_{\mathrm{a}'} \frac{x_{\mathrm{a}'} x_{\mathrm{c}} G_{\mathrm{ac,a'c}}}{\sum_k x_k G_{k\mathrm{c,a'c}}} \left(\tau_{\mathrm{ac,a'c}} - \frac{\sum_{k \neq \mathrm{c}} x_k G_{k\mathrm{c,a'c}} \tau_{k\mathrm{c,a'c}}}{\sum_{k \neq \mathrm{c}} x_k G_{k\mathrm{c,a'c}}} \right)}{\sum_{\mathrm{a}''} x_{\mathrm{a}''}} \tag{22}$$

where,

$$\tau_{\mathrm{ma,ca}} = \tau_{\mathrm{am}} - \tau_{\mathrm{ca,m}} + \tau_{\mathrm{m,ca}} \tag{23}$$

$$\tau_{\mathrm{am}} = -\ln \frac{G_{\mathrm{am}}}{\alpha_{\mathrm{am}}} \tag{24}$$

$$G_{\mathrm{am}} = \frac{\sum_{\mathrm{c}} x_{\mathrm{c}} G_{\mathrm{ca,m}}}{\sum_{\mathrm{c}} x_{\mathrm{c}}} \tag{25}$$

$$\alpha_{\mathrm{am}} = \frac{\sum_{\mathrm{c}} x_{\mathrm{c}} \alpha_{\mathrm{ca,m}}}{\sum_{\mathrm{c}} x_{\mathrm{c}}} \tag{26}$$

$$\tau_{\mathrm{mc,ac}} = \tau_{\mathrm{cm}} - \tau_{\mathrm{ca,m}} + \tau_{\mathrm{m,ca}} \tag{27}$$

$$\tau_{\mathrm{cm}} = -\ln \frac{G_{\mathrm{cm}}}{\alpha_{\mathrm{cm}}} \tag{28}$$

$$G_{\mathrm{cm}} = \frac{\sum_{\mathrm{a}} x_{\mathrm{a}} G_{\mathrm{ca,m}}}{\sum_{\mathrm{a}} x_{\mathrm{a}}} \tag{29}$$

$$\alpha_{\mathrm{cm}} = \frac{\sum_{\mathrm{a}} x_{\mathrm{a}} \alpha_{\mathrm{ca,m}}}{\sum_{\mathrm{a}} x_{\mathrm{a}}} \tag{30}$$

$$G = e^{-\alpha\tau} \tag{31}$$

Eqs. (18), (19), (21), and (22) are in the symmetrical convention. For ions, they can be converted into the rational unsymmetrical and molality conventions according to Eqs. (1) and (2).

The α parameters are interchangeable, i.e., $\alpha_{ij} = \alpha_{ji}$. In this work, there are only one cation and one anion in each mixture. Thus, the salt-salt parameters, $\tau_{\mathrm{ca,c'a}} = \tau_{\mathrm{ca,c'}}$ and $\tau_{\mathrm{ac,a'c}} = \tau_{\mathrm{ac,a'}}$, are not relevant here. The adjustable parameters are $\alpha_{\mathrm{water,alcohol}}$, $\alpha_{\mathrm{water,salt}}$, $\alpha_{\mathrm{alcohol,salt}}$, $\tau_{\mathrm{water,alcohol}}$, $\tau_{\mathrm{alcohol,water}}$, $\tau_{\mathrm{water,salt}}$, $\tau_{\mathrm{salt,water}}$, $\tau_{\mathrm{alcohol,salt}}$, and $\tau_{\mathrm{alcohol,salt}}$. In short, these parameters are noted as α_{wa}, α_{ws}, α_{as}, τ_{wa}, τ_{aw}, τ_{ws}, τ_{sw}, τ_{as}, and τ_{as}. $\alpha_{\mathrm{wa}} = 0.3$, $\alpha_{\mathrm{ws}} = 0.2$, and $\alpha_{\mathrm{as}} = 0.2$ are taken according to common practice [27]. There is no adjustable parameter in the PDH and Born terms. Therefore, the remaining adjustable parameters are the τ parameters. In addition, a temperature dependence is introduced for τ:

$$\tau = \tau_0 + \tau_1 \left(\frac{1}{T} - \frac{1}{T_0}\right) \tag{32}$$

where τ_0 is obtained at T_0, at which isothermal datasets are usually available, typically at 298.15 K, while τ_1 is obtained with datasets at other temperatures.

3.2 Is consistency an issue?

Because that the difference between the consistent and original E-NRTL models is only with solvent composition derivatives, and that MIAC only involves ion composition derivatives, the consistent modification has no impact on MIAC. Thus, the parameters of the consistent and original E-NRTL models are identical for OF-M. Table 1 shows the ADs and MDs of the consistent and original E-NRTL models with OF-M and OF-MV. For vapor pressure, the relative deviation is taken (see Eq. (9)). For vapor phase molar fraction and MIAC, the absolute deviation is taken, because these data are in general between 0 and 1, and thus the relative deviations are exaggerated when the values are small. In the cases with OF-M, VLE is predicted. For the methanol mixtures, with OF-M, the consistent E-NRTL model predicts both VLE p and y more accurately than the original model; with OF-MV, there is no significant difference between the consistent and original E-NRTL models. For the ethanol mixtures, however, with either OF-M or OF-MV, the difference

between the consistent and original E-NRTL models is not significant in terms of the ADs and MDs of MIAC and VLE.

Table 1. Average deviations (ADs) and maximum deviations (MDs) of the consistent and original E-NRTL models with OF-M (MIAC) and OF-MV (MIAC and VLE). The prediction deviations are presented in italic and blue. Temperature and composition ranges of the experimental datasets are provided in Table 4. Ion composition is cut off at $x_{\mathrm{ion}} = 0.06$.

Mixture	Property	Reference	Consistent, OF-M		Consistent, OF-MV		Original, OF-M		Original, OF-MV	
			100AD	100MD	100AD	100MD	100AD	100MD	100AD	100MD
(water + methanol + NaCl)	MIAC	Xu et al. 2014 [66]	0.56	1.4	0.60	1.4	0.56	1.4	0.64	1.5
		Basili et al. 1996 [67]	1.4	5.0	1.5	6.0	1.4	5.0	1.5	6.7
	VLE	Yang & Lee 1998 [68], *p*	*6.0*	*12*	2.2	5.5	*8.2*	*14*	2.2	5.5
		y	*2.8*	*6.2*	1.1	2.3	*4.2*	*8.0*	1.1	2.3
(water + methanol + KCl)	MIAC	Basili et al. 1997 [69]	1.1	4.2	1.2	4.5	1.1	4.2	1.2	4.6
	VLE	Yang & Lee 1998 [68], *p*	*3.3*	*7.4*	1.8	4.3	*4.5*	*8.7*	1.7	4.3
		y	*1.4*	*3.1*	0.48	0.91	*2.1*	*4.1*	0.46	0.86
(water + ethanol + NaCl)	MIAC	Esteso et al. 1989 [70]	2.4	7.2	2.4	7.2	2.4	7.2	2.5	7.3
		Mamontov et al. 2016 [71] [a]	0.91	2.7	0.91	2.9	0.91	2.7	1.0	3.5
	VLE	Yang et al. 1979 [46], *p*	*2.1*	*5.5*	2.2	6.5	*1.8*	*4.4*	2.0	6.0
		y	*1.9*	*3.4*	1.6	3.3	*2.8*	*4.3*	1.8	3.5
(water + ethanol + KCl)	MIAC	Mussini et al. 1995 [72]	0.88	1.7	0.88	1.8	0.88	1.7	0.90	1.7
	VLE	Yang et al. 1979 [46], *p*	*2.0*	*3.7*	2.4	4.0	*0.98*	*2.6*	2.3	4.0
		y	*1.9*	*2.8*	1.7	2.6	*2.6*	*3.7*	1.8	2.8

Note: [a] The dataset includes data at other temperatures. Deviations in this table are for the 298.15 K part of the dataset.

However, the more significant differences in trends are masked by the AD and MD values. Figure 4 shows the comparison of the solvent activity coefficients of (water + methanol + NaCl) calculated using the consistent and original E-NRTL models with OF-M and OF-MV. The line types denote the different models. The colors denote the salt compositions. The lines and dots in the upper part of the graph are alcohol activity coefficient, while those in the lower part are water activity coefficient. The latter is close to unity for all the mixtures in the entire data ranges, and does not represent a good criterion against the models. Thus, here the analysis focuses on the alcohol activity coefficient. Figures for (water + methanol + KCl), (water + ethanol + NaCl/KCl) are provided in the Supporting Information. With OF-MV, the results calculated with the consistent and original E-NRTL models almost overlap. With OF-M, the results calculated with the consistent E-NRTL model is closer to the experimental data compared to the original model for all the mixtures. Therefore, although not to the level of the OF-MV results, VLE is predicted more accurately with the consistent model compared to the original model, when only MIAC is available, which is often the case as shown in the data summary in Section 6. A table is provided in the Supporting Information for the parameters. For all the mixtures, the parameters regressed with OF-M and OF-MV are closer for the consistent model compared to the original, which confirms that the MIAC and VLE properties are better reconciled when calculated using the consistent E-NRTL model. In addition, the alcohol activity coefficient of the methanol mixtures present larger deviations with OF-M. Figure 5 shows the vapor pressure of (water + methanol + NaCl) with 10% and 30% weight fraction methanol (salt-free basis) with OF-M and OF-MV at 298.15 K. As salt composition increases, the experimental vapor pressure increases, i.e., the salting out behavior dominates vapor pressure change even at this low alcohol composition; the consistent and original E-NRTL models with OF-MV capture this behavior; while the models with OF-M fail to capture this behavior, which results in the comparatively larger deviations as shown in Table 1.

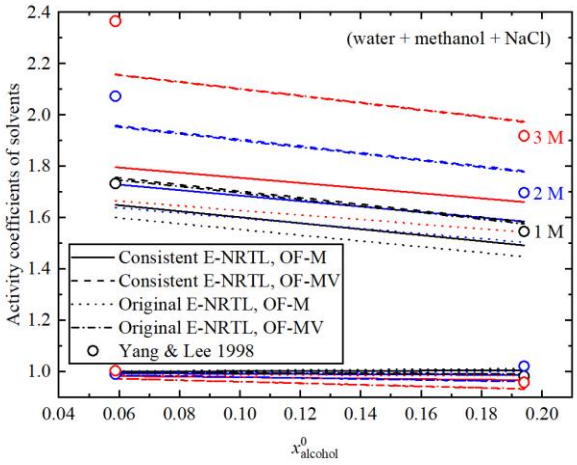

Figure 4. Comparison of the solvent activity coefficients of (water + methanol + NaCl) calculated using the consistent and original E-NRTL models with OF-M and OF-MV at 298.15 K. The upper part of the graph is alcohol activity coefficient, while the lower part is water activity coefficient. The experimental data is from reference [68].

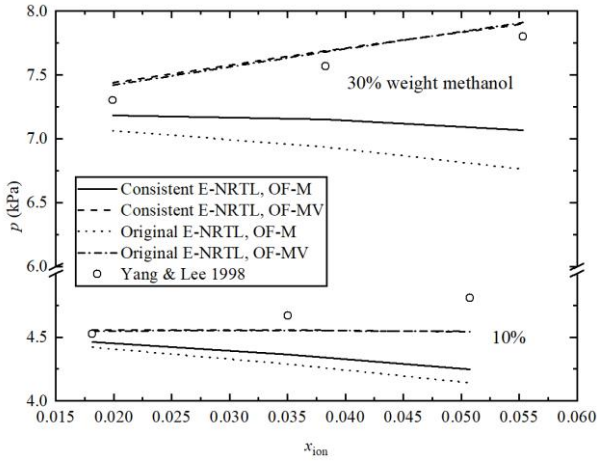

Figure 5. Vapor pressure of (water + methanol + NaCl) with 10% and 30% weight fraction methanol (salt-free basis) with OF-M and OF-MV at 298.15 K. The experimental data is from reference [68].

To sum up, with OF-MV, there is no significant difference between the consistent and original E-NRTL models; with OF-M, the consistent E-NRTL model is more accurate than the original model, in terms of both VLE results and trends of solvent activity coefficients. In the following context, unless specifically noted, the consistent E-NRTL model is analyzed; "E-NRTL" refers to the consistent model.

3.3 E-NRTL at larger salt composition

This section investigates how the E-NRTL model extrapolates to larger salt composition. The aim is to find a cut-off salt composition that can be used in data selection, rather than to obtain

accurate results in as large range as possible. We find that the E-NRTL model is not accurate for both aqueous and mixed-solvent electrolyte solutions at large salt composition.

Results of (water + salt) binary mixtures are shown rather than those of (water + alcohol + salt) ternary mixtures, because the former are confirmed by experimental data from various sources. Figures 6 and 7 show the deviations of vapor pressure calculated with the E-NRTL model with OF-MV and parameters regressed in the region up to $x_{\mathrm{ion}} = 0.06$ and in the entire x_{ion} range for (water + NaCl) and (water + LiCl). Results for MIAC is not significantly different within $x_{\mathrm{ion}} = 0.06$ and is presented in the Supporting Information. References for the experimental datasets are provided in the Supporting Information. The red and blue dots are the same datasets compared with the E-NRTL model using different parameters. In this work, all electrolyte solution data (MIAC and VLE, aqueous and mixed-solvent) are cut off at $x_{\mathrm{ion}} = 0.06$ when parameters are regressed. There are three scenarios following this cut off. For salts with low solubility, e.g., KCl and NaF, the cut off covers all or most of the solubility range. Thus, the cut off x_{ion} is close to the solubility limit, i.e., the parameters regressed up to $x_{\mathrm{ion}} = 0.06$ applies up to the solubility limit. For salts with solubility that is moderately larger than $x_{\mathrm{ion}} = 0.06$, e.g., NaCl, MIAC and VLE calculated with parameters regressed up to $x_{\mathrm{ion}} = 0.06$ are slightly more accurate at lower salt composition compared to those calculated with parameters regressed in the entire x_{ion} range (approximately up to $x_{\mathrm{ion}} = 0.09$); however, deviations increase drastically beyond $x_{\mathrm{ion}} = 0.06$ and reach 0.15 at $x_{\mathrm{ion}} = 0.09$, while the deviation of MIAC calculated with parameters regressed in the entire x_{ion} range is within 0.05 at $x_{\mathrm{ion}} = 0.09$; for vapor pressure, the increase of deviation is much smaller in the large x_{ion} range compared to that of MIAC, being slightly larger than 3% at the solubility limit. When regressed to MIAC and VLE data in the entire composition range, the obtained parameters are exactly the same as those reported by Yan and Chen [73], i.e., $\tau_{sw} = -4.54$, $\tau_{ws} = 8.86$. For salts with solubility that is much larger than $x_{\mathrm{ion}} = 0.06$, e.g., LiCl, however, although VLE is included in the objective function along with MIAC, regression in the entire x_{ion} range results in large deviation in vapor pressure (up to 50%) in both low and high salt composition ranges. To sum up, regression to the entire x_{ion} range can improve accuracy in the high salt composition range for salts with solubility that is moderately larger than $x_{\mathrm{ion}} = 0.06$, but cannot for salts with solubility that is much larger than $x_{\mathrm{ion}} = 0.06$ (e.g., LiCl); in both cases, accuracy in the low salt composition range is worse compared to that calculated using parameters regressed up to $x_{\mathrm{ion}} =$

0.06. It is necessary to account for model capability when selecting the range of data used in parameter regression rather than use everything available. Furthermore, salts present very different solubility, while cutting off at certain x_{ion} provides a common ground that facilitates finding parameter trends. Therefore, although the deviations are larger at the high salt composition for the (water + NaCl) case, it is still decided that all data are cut off at $x_{\mathrm{ion}} = 0.06$. The model is here used to obtain a guide for data selection, rather than to obtain accurate results in large ranges.

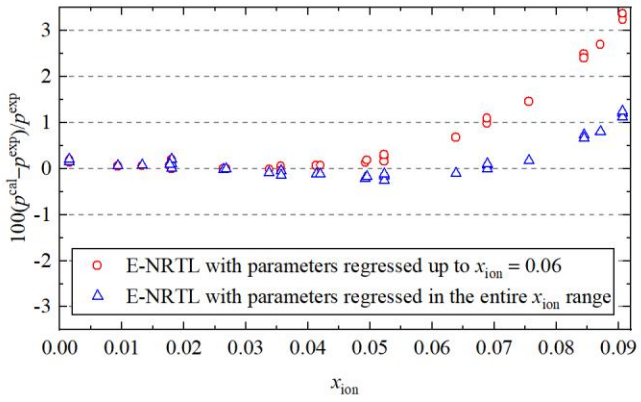

Figure 6. Deviations from experimental data of vapor pressure calculated with the E-NRTL model with OF-MV and parameters regressed in the region up to $x_{\mathrm{ion}} = 0.06$ and in the entire x_{ion} range for (water + NaCl). References for the experimental datasets are provided in the Supporting Information.

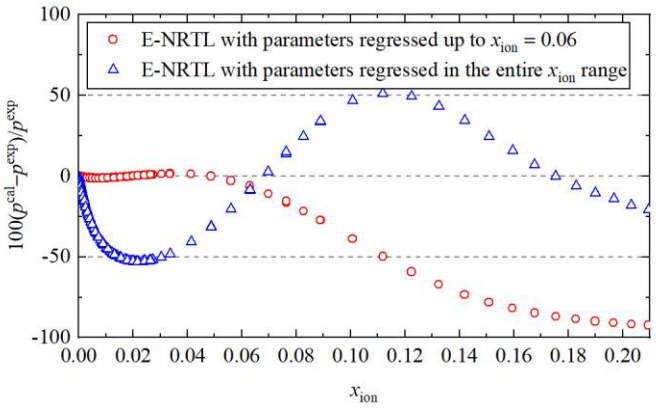

Figure 7. Deviations from experimental data of vapor pressure calculated with the E-NRTL model with OF-MV and parameters regressed in the region up to $x_{\mathrm{ion}} = 0.06$ and in the entire x_{ion} range for (water + LiCl). References for the experimental datasets are provided in the Supporting Information.

4 Data consistency analysis

This section presents results for the data consistency analysis. The impact of the objective functions (Section 4.1) and the selection of water-salt parameters (Section 4.2) are discussed. Then, the determination of the alcohol-salt parameters and the ternary results (Section 4.3) are shown.

4.1 Impact of the objective functions

In this section, the impact of the objective functions are analyzed. OF-M, OF-V, and OF-MV are compared. In Table 2, the three objective functions are tested on (water + ethanol + NaCl). The resulting deviations on MIAC and VLE are evaluated. For OF-M, VLE results are predicted. For OF-V, MIAC results are predicted. The analysis is performed with two sets of water-salt parameters and different upper and lower bounds for the alcohol-salt parameters. Let us first focus on the 1st water-salt parameter set, which is the recommended set. The 2nd parameter set will be discussed in Section 4.2. Alcohol-salt parameters are optimized in two ranges [(– 5, – 1), (4, 12)] and [(4, 16), (4, 8)] (extended when boundaries are reached in optimizations), which are found to be reasonable ranges using a trial-and-error procedure.

One can observe that different optimal parameter sets could be found when different parameter ranges are imposed, indicating possible local minima in the OFs. In Table 2, results calculated with OF-M and OF-MV are approximately as good, only slightly better with the parameter set obtained in [(– 5, – 1), (4, 12)]. However, OF-V results in large deviations from the MIAC datasets, when parameters are regressed in both ranges. Therefore, in the cases that VLE is not available, VLE predictions are acceptable when using parameters regressed only based on MIAC; however, in the cases that MIAC is not available, MIAC predictions are likely to be far off when using parameters regressed only based on VLE.

Table 2. Alcohol-salt parameters regressed in different ranges and deviations of the E-NRTL model for (water + ethanol + NaCl) with two sets of water-salt parameters (1st set: $\tau_{sw} = -4.2915$, $\tau_{ws} = 8.2464$; 2nd set: $\tau_{sw} = -1.0391$, $\tau_{ws} = -4.4583$). The information provided in the column on the left of the parameter values are the ranges in which the parameters are regressed. AD stands for average deviation. MD stands for maximum deviation. Predicted values are shown in italic and blue. Objective functions are as defined in Section 2.4.

τ_{wa} & τ_{aw}	OF	τ_{sa}		τ_{as}		α	Esteso et al. [70]		Mamontov et al. [71]		Yang et al. [46] p		y	
							100AD	100MD	100AD	100MD	100AD	100MD	100AD	100MD
1st	M	(– 5, – 1)	– 1.8983	(4, 12)	7.6887	0.2	2.4	7.2	0.91	2.7	*2.1*	*5.5*	*1.9*	*3.4*
		(4, 16)	15.978	(4, 8)	6.0436	0.2	2.5	7.4	1.1	3.7	*4.7*	*12*	*1.4*	*3.5*
	V	(– 5, 1)	– 0.12873	(4, 12)	5.3666	0.2	*3.9*	*8.8*	*3.9*	*8.8*	2.1	6.6	1.6	3.3
		(4, 16)	15.996	(4, 8)	4.3070	0.2	*5.9*	*19*	*7.5*	*21*	2.1	6.3	1.6	3.3
	MV	(– 5, – 1)	– 1.4847	(4, 12)	7.2184	0.2	2.4	7.2	0.91	2.9	2.2	6.5	1.6	3.3
		(4, 16)	16.000	(4, 8)	5.9058	0.2	2.5	7.4	1.2	3.0	4.5	11	1.4	3.3
2nd	M	(1, 5)	3.4910	(– 5, 1)	– 3.1604	0.2	3.3	8.9	1.6	4.2	*1.3*	*3.3*	*2.2*	*3.7*
	V	(1, 5)	3.2014	(– 5, 1)	– 1.3305	0.2	*3.3*	*8.9*	*1.7*	*4.3*	2.0	5.5	1.8	3.5
	MV	(1, 5)	3.5471	(– 5, 1)	– 1.8342	0.2	3.3	8.9	1.7	4.2	1.9	5.1	1.9	3.5

4.2 Selection of water-salt parameters

Modeling the aqueous electrolyte solutions is "simple". Usually, a few sets of parameters result in approximately the same accuracy level. However, these parameters are not as good when extended to mixed-solvent electrolyte solutions. In Table 2, an example is provided for the (water + ethanol + NaCl) case. The optimal alcohol-salt parameters and ternary results calculated with the E-NRTL model and two sets of water-salt parameters are presented. The 1st water-salt parameter set is ($\tau_{\mathrm{sw}} = -4.2915$, $\tau_{\mathrm{ws}} = 8.2464$). The 2nd water-salt parameter set is ($\tau_{\mathrm{sw}} = -1.0391$, $\tau_{\mathrm{ws}} = -4.4583$). The 1st water-salt parameter set is regressed in a range that is close to the values reported by Chen's group [27,54]. The 2nd parameter set is regressed in a different range. They are approximately as accurate for representing VLE and MIAC of the (water + NaCl) binary mixture. However, for the (water + ethanol + NaCl) ternary mixture, for both OF-M and OF-MV, the 2nd parameter set is less accurate for representing ternary MIAC, although approximately as accurate for the VLE dataset. Furthermore, the alcohol-salt parameter set is very different for the two water-salt parameter sets. Thus, the optimal parameters for the water-salt and alcohol-salt pairs are not independent. Therefore, in this work, parameters are regressed near the water-NaCl parameters as a first attempt for all the other water-salt pairs, which turns out to work very well.

4.3 Alcohol-salt parameters and ternary results

Table 3 shows the regressed parameters of the E-NRTL model for the (water + methanol/ethanol + alkali halide) mixtures. Parameters are regressed according to Eq. (9). Water-alcohol parameters are regressed to OF-V. Water-salt and alcohol-salt parameters are regressed to OF-M or OF-MV, depending on the data availability and reliability. The used (water + salt) datasets are summarized in the Supporting Information. Information of the used (water + alcohol + salt) datasets are summarized in Table 4. In many cases, reliable MIAC data are available at 298.15 K. Thus, $\tau_{0,\mathrm{solvent-salt}}$ and $\tau_{0,\mathrm{salt-solvent}}$ are first regressed; then, if reliable data are available at other temperatures, the temperature gradients, $\tau_{1,\mathrm{solvent-salt}}$ and $\tau_{1,\mathrm{salt-solvent}}$, are regressed. When data are not available at 298.15 K, the τ_0 and τ_1 parameters are regressed together. The water-salt parameters are regressed to (water + salt) data, while the alcohol-salt parameters are regressed to (water + alcohol + salt) data. As we have shown in Section 4.1, OF-M and OF-MV can be used in parameter regression, while OF-V results in large deviations in MIAC predictions. For most of the listed mixtures, MIAC data are available. Solvent-salt parameters that are regressed to OF-M and

OF-MV are marked as bold in the table. In some cases, only VLE data are available; the solvent-salt parameters are regressed to OF-V, and are marked as green in the table. In a few cases for the mixed-solvent electrolyte mixtures, all the available datasets are decided to be unreliable after evaluation; the parameters are marked as blue and italic in the table. In some cases, data are only available at 298.15 K; no temperature gradient is given in the table. No trend is observed within the parameters. However, for all the water-salt pairs, the parameters are within a small range; for the alcohol-salt pairs, the parameters are more scattered, likely because of the lower consistency of the experimental datasets of the (water + alcohol + salt) ternary mixtures compared to those of the (water + salt) binary mixtures.

The overall average deviations (ADs) of the E-NRTL model from experimental datasets are presented in Table 5 along with results calculated using the other parameterization strategies. The ADs and maximum deviations (MDs) for each dataset are presented in the Supporting Information. Deviations are only shown for the mixtures for which the parameters that are regressed to OF-M and OF-MV. Temperature and composition ranges of the entire dataset are also shown. The datasets are only compared up to $x_{\mathrm{ion}} = 0.06$ and T = 400 K. The behavior of the model beyond the composition range has been discussed in Section 3.3. The impact of temperature is captured by the temperature gradient introduced in Eq. (32), by the temperature dependence of the pure fluid density and relative permittivity, and by the temperature dependence in the model formulation. The two temperature gradient parameters do not present any trend, even though VLE data at different temperatures are included in the regressions. Parameter degeneracy is observed between the two temperature gradients. Figure 8 shows the comparison of MIAC calculated using the E-NRTL model and the experimental data for (water + ethanol + NaCl). The agreement between the experimental datasets from different sources, and between the datasets and the E-NRTL model, confirms the reliability of the evaluated experimental data, as well as that of the regressed parameters.

Table 3. Parameters of the E-NRTL model for the (water + methanol/ethanol + alkali halide) mixtures. Water-alcohol parameters are regressed to OF-V. Water-salt and alcohol-salt parameters are regressed to OF-M or OF-MV, depending on the data availability and reliability. The used (water + salt) datasets are summarized in the Supporting Information. The relevant (water + alcohol + salt) datasets are summarized in Table 4. Solvent-salt parameters that are regressed to OF-M and OF-MV are marked as bold. Parameters that are determined based on unreliable (uncertain) datasets are marked as italic and blue. Solvent-salt parameters that are regressed to OF-V are marked as green.

Binary pair (*i*-*j*)	α	A			
		$\tau_{0,ji}$	$\tau_{0,ij}$	$\tau_{1,ji}$	$\tau_{1,ij}$
Water-methanol	0.3	0.21334	0.29399	1175.2	– 1900.8
Water-ethanol	0.3	0.079833	1.4142	347.97	– 634.43
Solvent-salt parameters that are regressed to OF-M and OF-MV.					
Water-LiCl	**0.2**	**– 4.9031**	**9.3612**	**– 299.61**	**608.71**
Water-NaCl	**0.2**	**– 4.2915**	**8.2464**	**– 111.94**	**604.96**
Water-KCl	**0.2**	**– 4.0036**	**7.8180**	**– 550.87**	**1628.3**
Water-RbCl	**0.2**	**– 4.0639**	**8.0359**	**– 20.506**	**334.38**
Water-CsCl	**0.2**	**– 4.3330**	**8.7956**	**– 102.70**	**424.63**
Water-NaF	**0.2**	**– 4.5064**	**9.0168**	**/**	**/**
Water-LiBr	**0.2**	**– 5.0894**	**9.7570**	**685.09**	**– 2848.1**
Water-NaBr	**0.2**	**– 4.5219**	**8.6862**	**20.843**	**122.11**
Water-KBr	**0.2**	**– 4.0552**	**7.8781**	**332.36**	**– 998.97**
Water-CsBr	**0.2**	**– 4.2563**	**8.6560**	**53.154**	**– 212.31**
Water-NaI	**0.2**	**– 4.6495**	**8.8420**	**– 101.08**	**434.72**
Water-KI	**0.2**	**– 3.9659**	**7.5374**	**– 83.600**	**250.09**
Methanol-LiCl	**0.2**	**– 4.2412**	**9.0090**	**– 755.47**	**4409.9**
Methanol-NaCl	**0.2**	**– 2.4187**	**6.8712**	**563.09**	**1775.6**
Methanol-KCl	**0.2**	**– 2.6033**	**7.7412**	**– 1350.1**	**5212.9**
Methanol-RbCl	**0.2**	**– 2.8102**	**7.5196**	**/**	**/**
Methanol-NaF	**0.2**	**– 4.7905**	**15.000**	**/**	**/**
Ethanol-NaCl	**0.2**	**– 1.4847**	**7.2184**	**– 19.615**	**2077.0**
Ethanol-KCl	**0.2**	**– 0.10247**	**6.9013**	**2211.8**	**3698.4**
Ethanol-CsCl	**0.2**	**– 1.5844**	**7.4986**	**/**	**/**
Ethanol-NaF	**0.2**	**1.5302**	**14.980**	**/**	**/**
Parameters that are determined based on unreliable (uncertain) datasets.					
Methanol-CsCl	*0.2*	*– 3.3776*	*9.5764*	*/*	*/*

Binary pair (*i*-*j*)	α	A			
		$\tau_{0,ji}$	$\tau_{0,ij}$	$\tau_{1,ji}$	$\tau_{1,ij}$
Methanol-NaBr	*0.2*	*– 3.2938*	*6.8686*	*/*	*/*
Methanol-CsBr	*0.2*	*– 4.8626*	*13.080*	*/*	*/*
Ethanol-LiCl	*0.2*	*– 2.9328*	*7.9705*	*/*	*/*
Ethanol-NaBr	*0.2*	*– 1.6454*	*6.4317*	*2788.69*	*– 374.35*
Solvent-salt parameters that are regressed to OF-V.					
Ethanol-KBr	0.2	– 2.9567	6.0368	– 646.38	642.01
Ethanol-NaI	0.2	– 3.4167	7.0721	/	/
Ethanol-KI	0.2	– 1.5412	1.9649	– 703.52	– 952.12

498 Table 4. Summary of the experimental datasets for the (water + methanol/ethanol + alkali halide)
499 mixtures. The significance of the letters under "group" is explained in Section 5.2.

Reference	Group	T (K)	Max(x_{ion})	w^0_{alc}	N_{DP}
(water + methanol + LiCl)					
MIAC					
Harned 1962 [74]	**T**	298.15	0.037	0.100 – 0.200	18
Mussini et al. 2000 [45]	**T**	298.15	0.131	0.200 – 0.800	128
Basili et al. 1999 [75]	**T**	298.15	0.131	0.200	12
Hu et al. 2008 [76]	**T**	298.15	0.027	0.050 – 0.150	46
VLE					
Broul et al. 1969 [77]	**T**	333.15	0.179	0.010 – 0.892	40
(water + methanol + NaCl)					
MIAC					
Xu et al. 2014 [66]	**R**	298.15	0.022	0.100	28
Basili et al. 1996 [67]	**R**	298.15	0.068	0.200 – 0.800	76
Yao et al. 1999 [78]	**R**	308.15 – 318.15	0.038	0.100 – 0.900	206
Hernandez-Hernandez et al. 2007 [79]	**R**	308.15	0.035	0.100	17
VLE					
Yang & Lee 1998 [68]	**R**	298.15	0.065	0.100 – 0.300	7
Yao et al. 1999 [80]	**R**	318.15	0.090	0.110 – 0.949	30
Johnson & Furter 1960 [81]	**R**	339.25 – 352.15	0.092	0.050 – 0.928	12
(water + methanol + KCl)					
MIAC					
Basili et al. 1997 [69]	**R**	298.15	0.037	0.200 – 0.600	47

Reference	Group	T (K)	Max(x_{ion})	w^0_{alc}	N_{DP}
Harned 1962 [74]	**T**	298.15	0.037	0.100 – 0.200	18
VLE					
Yang & Lee 1998 [68]	**R**	298.15	0.029	0.100 – 0.300	6
Johnson & Furter 1960 [81]	**R**	338.45 – 351.55	0.095	0.042 – 0.944	12
(water + methanol + RbCl)					
MIAC					
Zhang et al. 2004 [82]	**R**	298.15	0.043	0.100	9
Basili et al. 1997 [69]	**R**	298.15	0.068	0.200 – 0.800	67
(water + methanol + CsCl)					
MIAC					
Hu et al. 2007 [83]	**U**	298.15	0.029	0.100 – 0.400	72
Cui et al. 2007 [84]	**U**	298.15	0.061	0.100 – 0.400	64
Falciola et al. 2006 [85]	**U**	298.15	0.018	0.250 – 0.750	54
(water + methanol + NaF)					
MIAC					
Hernandez-Luis et al. 2003 [86]	**R**	298.15	0.010	0.100 – 0.900	113
VLE					
Boone et al. 1976 [87]	**U**	338.95 – 368.65	0.028	0.047 – 0.953	25
(water + methanol + NaBr)					
MIAC					
Han & Pan 1993 [88]	**U**	298.15	0.064	0.100 – 0.900	108
VLE					
Yang & Lee 1998 [68]	**T**	298.15	0.097	0.236 – 0.423	5
Boone et al. 1976 [87]	**U**	338.95 – 370.55	0.095	0.042 – 0.959	23
(water + methanol + CsBr)					
MIAC					
Falciola et al. 2006 [85]	**U**	298.15	0.018	0.250 – 0.750	54
(water + methanol + CsI)					
MIAC					
Falciola et al. 2006 [85]	**U**	298.15	0.018	0.250 – 0.750	54
(water + ethanol + LiCl)					
MIAC					
Hu et al. 2008 [76]	**U**	298.15	0.026	0.050 – 0.150	42

Reference	Group	T (K)	Max(x_{ion})	w^0_{alc}	N_{DP}
Hernandez-Luis et al. 2008 [89]	**U**	298.15	0.097	0.200 – 0.800	64
VLE					
Shaw & Butler 1930 [90]	**U**	298.15	0.133	0.148 – 0.992	24
(water + ethanol + NaCl)					
MIAC					
Esteso et al. 1989 [70]	**R**	298.15	0.038	0.200 – 0.900	123
Mamontov et al. 2016 [71]	**R**	288.15 – 318.15	0.055	0.100 – 0.400	117
VLE					
Yang et al. 1979 [46]	**R**	298.15	0.025	0.100 – 0.700	22
Meyer et al. 1991 [91]	**T**	306.35 – 332.05	0.072	0.013 – 0.904	30
(water + ethanol + KCl)					
MIAC					
Mussini et al. 1995 [72]	**R**	298.15	0.038	0.200 – 0.400	24
VLE					
Yang et al. 1979 [46]	**R**	298.15	0.021	0.100 – 0.600	14
Sun 1996 [92]	**R**	352.2 – 356.1	0.029	0.378 – 0.714	10
(water + ethanol + CsCl)					
MIAC					
Mussini et al. 1995 [72]	**T**	298.15	0.112	0.200 – 0.700	59
(water + ethanol + NaF)					
MIAC					
Hernandez-Luis et al. 2003 [86]	**T**	298.15	0.011	0.100 – 0.800	89
(water + ethanol + LiBr)					
VLE					
Sun 1996 [92]	**U**	352.51 – 356.07	0.050	0.378 – 0.714	12
(water + ethanol + NaBr)					
MIAC					
Gonzalez-Diaz et al. 1995 [93]	**U**	298.15	0.027	0.200 – 0.998	100
Han & Pan 1993 [88]	**U**	298.15	0.083	0.100 – 0.900	120
VLE					
Sun 1996 [92]	**U**	351.46 – 356.15	0.049	0.378 – 0.856	22
(water + ethanol + KBr)					
VLE					

Reference	Group	T (K)	Max(x_{ion})	w^0_{alc}	N_{DP}
Burns & Furter 1976 [94]	**T**	354.65 – 356.75	0.090	0.399 – 0.536	35
(water + ethanol + CsBr)					
MIAC					
Du et al. 2012 [95]	**U**	298.15	0.019	0.100 – 0.300	57
(water + ethanol + NaI)					
VLE					
Yamamoto et al. 1995 [96]	**T**	298.15	0.052	0.140 – 0.968	9
(water + ethanol + KI)					
VLE					
Sun 1996 [92]	**U**	351.63 – 356.05	0.038	0.533	15
Burns & Furter 1979 [97]	**T**	355.25 – 357.15	0.106	0.384 – 0.856	21

Table 5. Overall ADs of the E-NRTL model from the experimental datasets

	100ADs	
	(water + methanol + salt) mixtures	(water + ethanol + salt) mixtures
MIAC	1.3	1.9
VLE, p	2.0	2.4
y	0.86	1.7

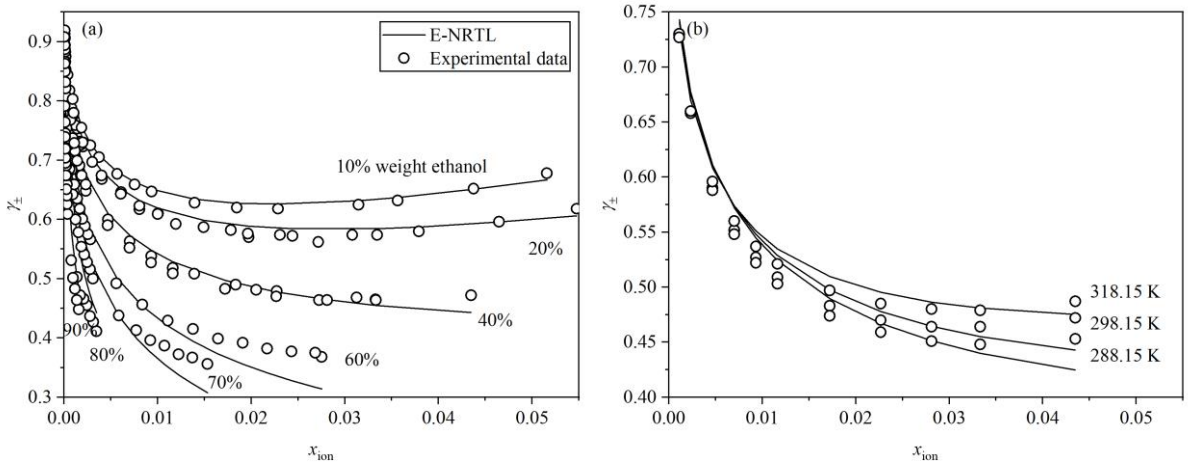

Figure 8. Comparison of MIAC calculated using the E-NRTL model and the experimental data [70,71] for (water + ethanol + NaCl): (a) 298.15 K at different ethanol compositions, (b) 40% weight fraction (salt-free basis) of ethanol at different temperatures

5 Benchmark database

In this section, the benchmark databases of the aqueous and mixed-solvent electrolyte solutions are presented.

5.1 Database for aqueous electrolyte solutions

Compared to the data status of the mixed-solvent electrolyte solutions, that of the aqueous electrolyte binary mixtures is much more extensive, which facilitates selection of the datasets that are validated in higher accuracy. Thus, only the selected datasets are shown here. The accepted MIAC and VLE datasets of the (water + salt) mixtures are summarized in the Supporting Information. The maximum x_{ion} column in the summary table shows the maximum value in the entire dataset. However, only the part that is smaller than $x_{ion} = 0.06$ is used in the regression and comparison, because the E-NRTL model deviates significantly from experimental values at large salt composition, as discussed in Section 3.3.

5.2 Database for mixed-solvent electrolyte solutions

The MIAC and VLE datasets of the (water + alcohol + salt) mixed-solvent electrolyte solutions are summarized in Table 4. Compared to the data status of the aqueous electrolyte solutions, that of the mixed-solvent electrolyte solutions is much less extensive. In some cases, there is only one dataset, or there are datasets that are contradictory to each other, so that they cannot be verified. Therefore, datasets are marked as "**R**" (recommended), "**T**" (tentative), and "**U**" (unknown). Group **R** denotes datasets that have been verified against other datasets with deviations within a few percent, e.g., the datasets of (water + methanol + NaCl). In many cases, such verifications are not possible, because data are scarce or contradictory between difference sources. In these cases, when there is only one dataset for the mixture, group **T** denotes datasets that are considered reliable by us, based on data trends and ranges, while group **U** denotes datasets that are considered unreliable by us. When there are multiple datasets available for the mixture, group **T** denotes datasets that deviate from each other but not by too much, while group **U** denotes datasets that deviate from each other by a lot so that it is not possible to decide which one or ones are reliable. As discussed in Section 2.1, experimental literature does not report the combined uncertainty of MIAC. For group **R** datasets, data from different sources agree with each other within a few percent; in most cases, one can expect the data to be very accurate. For group **T** datasets, discrepancy between data of different sources exceed 10% at boundaries of data ranges. For group **U** datasets, as no comparison can be made between data of different sources, accuracy cannot be estimated. The data tables are provided in the Supporting Information. Group **R** and **T** datasets are provided in the same file, while group **U** datasets are provided in a separate file. For

datasets that are marked as **T** and **U**, reasons are given in the following text in this section. These explanations are to be read together with the dataset summary in Table 4.

For (water + methanol + LiCl), although there are a few datasets, they do not agree with each other. The Hu et al. dataset [76] is smaller than the Harned dataset [74] by a few percent, while the datasets from the Mussini group [45,75] is larger by a few percent. A maximum deviation that is approximately 10% is observed in the only VLE dataset [77] as it is regressed along with the MIAC datasets. Therefore, these datasets are all marked as **T**. For this mixture, there is another MIAC dataset [98], which also covers a few other mixtures in Table 4. However, it is rejected because that scattering is up to a few percent within their own datasets for a few mixtures, and that these datasets do not agree with the **R** datasets that are available for some of these mixtures. There is another VLE dataset [87]. However, after regression, large deviations are observed for vapor phase molar fraction, which indicates that it is not reliable. Furthermore, datasets from the same reference are found to deviate significantly from the **R** datasets of a few other mixtures. Therefore, they are not included in the table.

For (water + methanol + NaCl), apart from the datasets summarized in Table 4, there are a few other datasets for MIAC and VLE [74,98–102]. However, the **R** datasets agree very well with each other. Therefore, these datasets are not included in the table. For MIAC, datasets from references [98,99] deviate significantly from the **R** datasets, while datasets from references [74,100,101] deviate from the **R** datasets by only a few percent. For VLE, there is another dataset [102]. However, the vapor phase molar fraction deviates significantly from the **R** datasets.

For (water + methanol + KCl), the Harned [74] dataset is marked as **T** because the Basili et al. [69] dataset agrees very well when regressed together with the VLE datasets [68,81], while it deviates by a few percent. Because the Basili et al. [69] MIAC dataset covers larger composition range, the Harned [74] dataset is not included in parameter regression. There are another MIAC dataset [98] and another VLE dataset [87]. However, they are not included in this table because they deviate from the **R** and **T** datasets significantly.

For (water + methanol + CsCl), the three available MIAC datasets [83–85] deviate significantly from each other. Therefore, no conclusion can be drawn and they are marked as **U**.

For (water + methanol + NaF), the Boone et al. VLE dataset [87] is marked as **U** because that it cannot be regressed to an accuracy within 10% even though NaF has a very low salt solubility, and that datasets from the same reference are found to deviate significantly from the **R** datasets of a few other mixtures.

For (water + methanol + NaBr), the MIAC dataset [88] and Boone et al. VLE dataset [87] are marked as **U**, because they deviate significantly when regressed together. Plotted on the graph (as shown in the Supporting Information), the MIAC data are clustered unreasonably: 40% ethanol weight fraction (salt-free basis) data are clustered with 60% data; while large gaps are present between the 20% and 40% data, and between the 60% and 80% data. Such behavior is not successfully correlated with the E-NRTL model. Thus, verifications against the **U** MIAC datasets cannot conclude on the reliability of the Yang and Lee VLE dataset [68]. However, datasets from the same reference have been verified for other mixtures. In addition, it is represented well with the E-NRTL model. Furthermore, the Yang and Lee dataset only covers small alcohol composition, and thus can be considered to be verified against the accepted (water + NaBr) datasets. Therefore, it is marked as **T**.

For (water + methanol + CsI), the Falciola et al. [85] dataset is the only available dataset, and thus cannot be verified. In addition, the Falciola et al. dataset present a strange behavior at high alcohol composition (75% weight fraction on the salt-free basis): at 0.018 ion-based molar fraction (approximately 0.5 M), MIAC increases to as large as 5. Such behavior is not observed in the (water + methanol + CsCl) and (water + methanol + CsBr) datasets and the lower-alcohol-composition part of the (water + methanol + CsI) dataset from the same reference, and cannot be represented with the E-NRTL model. Therefore, it is marked as **U**.

For (water + methanol + CsBr), the Falciola et al. [85] dataset is also marked as **U**. There is another dataset for this mixture by Du et al. [95]. However, MIAC decreases to very small values in the Du et al. [95] dataset. Such behavior is not observed in any of the **R** and **T** datasets of the investigated mixtures. Therefore, it is not included in Table 4.

For (water + ethanol + LiCl), the two MIAC datasets [76,89] and the VLE dataset [90] do not agree with each other. The 5%-15% ethanol weight fraction (salt-free basis) data from the Hu et al. [76] dataset is smaller than the 20% data from the Hernandez-Luis dataset [89], which is against the overall

trend that MIAC is smaller for the data at larger alcohol composition. Regression with the two MIAC datasets together with the VLE dataset does not result in any preference between them. In addition, there are two other VLE datasets [92,103]. However, they present vapor phase molar fraction that deviates significantly after regression, which is very unlikely for reliable data. Therefore, they are not included in the table. A dataset from reference [103] is also rejected after comparison with the recommended datasets for (water + ethanol + NaCl). However, datasets from reference [92] agrees well with the other **R** datasets for (water + ethanol + KCl) (marked as **R**), (water + ethanol + KI) (marked as **R**), and (water + ethanol + NaBr) (marked as **T** because the quality of other datasets of this mixture is not as good as that of the KCl and KI mixtures). In the meantime, being the only dataset for (water + ethanol + LiBr), a dataset from the same reference cannot be represented accurately after regression, and is marked as **U**.

For (water + ethanol + NaCl), in addition to the VLE dataset from reference [103], there is an additional MIAC dataset [104] that is not included in Table 4, because it deviates significantly from the **R** datasets. The Meyer et al. [91] dataset is marked as **T**, because its vapor phase molar fraction deviation is slightly larger than 10% after regression, while the other datasets agree very well with the model. Despite this, it is included in the table because it is the only VLE dataset at temperatures other than 298.15 K.

For (water + ethanol + CsCl), the Mussini et al. [72] dataset is marked as **T**. It is represented very well with the E-NRTL model. There is another MIAC dataset for this mixture by Hu et al. [83]. However, the data decreases to very small values at smaller than 0.008 ion-based molar fraction. Such behavior is not observed in any other investigated mixtures. A dataset from reference [83] is among the three MIAC datasets of (water + methanol + CsCl) that are contradictory to each other. In addition, a dataset from the same reference is rejected in the evaluation for the (water + CsCl) datasets, although not because of wrong trend, but rather only because of relatively larger deviations compared to the accepted datasets. Therefore, the Hu et al. [83] dataset is not included in Table 4.

For (water + ethanol + NaF), the Hernandez-Luis et al. dataset [86] is the only available dataset. Although it is not verified against other datasets, it is unlikely to be far off because of the very small solubility of NaF. In addition, it is very well represented with the E-NRTL model. Therefore, it is marked as **T**.

For (water + ethanol + NaBr), in the same range as the Gonzalez-Dias et al. dataset [93], the Han and Pan dataset [88] is slightly smaller. Furthermore, at larger salt composition, the upward curvature that seems quite artificial cannot be represented with the E-NRTL model. There is no dataset to verify the Han and Pan dataset, considering that the only VLE dataset is from a reference [92] in which datasets have been evaluated to be unreliable for a few other mixtures. In addition, a dataset is marked as **U** from the reference [88] for (water + methanol + NaBr). Therefore, the VLE dataset are marked as **T**, while the MIAC datasets are both marked as **U**. However, because no dataset of better quality is available, all three datasets have been used in the regression.

For (water + ethanol + KBr) and (water + ethanol + NaI), each mixture only has one VLE dataset [94,96]. Thus, they are not verified, but are represented very well with the E-NRTL model. Therefore, they are marked as **T**.

For (water + ethanol + CsBr), the only dataset is from reference [95]. It has the same problem as the (water + methanol + CsBr) from the same reference, presenting very small MIAC values that are not observed in any of the **R** and **T** datasets in the investigated mixtures. Therefore, it is marked as **U**.

For (water + ethanol + KI), there is another VLE dataset [105] that deviates significantly from the **T** dataset. It is not included in Table 4. The Sun [92] dataset deviates more compared to the **T** dataset after regression. Considering that datasets from the same reference also present larger deviations compared to the **R** datasets of other mixtures when more detailed comparisons are possible, the Sun [92] dataset is marked **U**. Therefore, the remaining VLE dataset cannot be verified, and is marked as **T**.

Figure 9 shows the data status of the (water + methanol/ethanol + alkali halide) ternary mixtures. As the datasets are evaluated, 13 of the 20 mixtures for which experimental data are available can be confirmed against data from other sources. From the perspectives of data quality and availability, we recommend that further experimental work be conducted on mixtures that only have **U** datasets (red), and on mixtures that have not been measured yet (white).

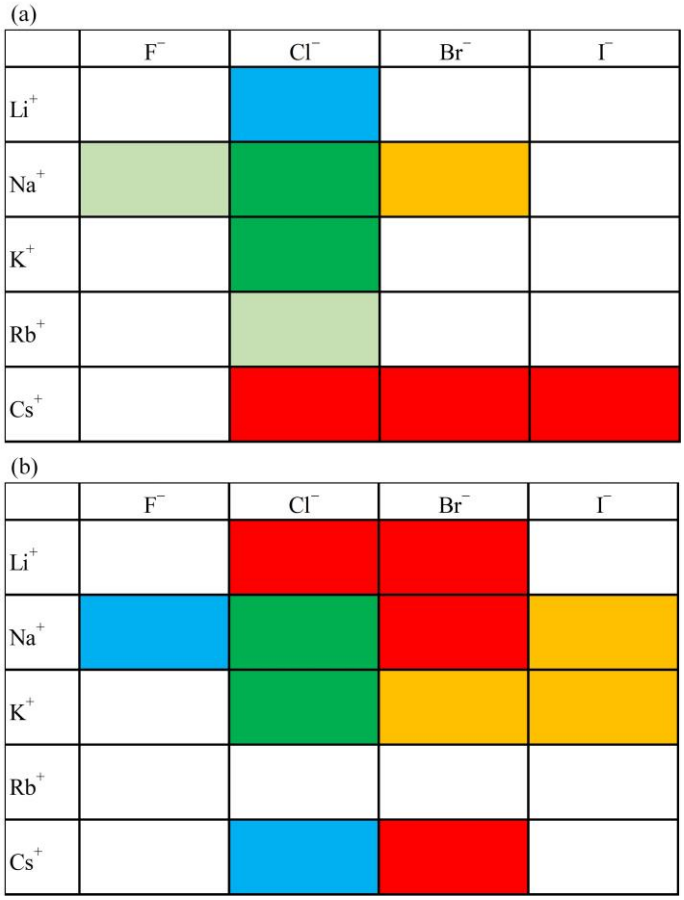

Figure 9. Data status of the ternary mixtures: (a) (water + methanol + alkali halide), (b) (water + ethanol + alkali halide). The green color denotes that there are **R** data for both MIAC and VLE. The light green color denotes that there are **R** data for MIAC only. The blue color denotes that there are **T** data for MIAC. The orange color denotes that there are **R** or **T** data for VLE only. The red color denotes that all available data are marked as **U**. The white color denotes that there are no data.

6 Conclusions and perspectives

In this work, a benchmark database for (water + methanol/ethanol + alkali halide) mixed-solvent electrolyte solutions is presented. A consistent E-NRTL model that satisfies the Gibbs-Duhem equation is utilized for data analysis, reconciling solvent and ion composition derivatives of the excess Gibbs energy, and thus reconciling MIAC and VLE. Major conclusions are:

1. Available experimental data of MIAC and VLE are comprehensively collected and critically evaluated for the 61 datasets of 20 solutions. The resulting benchmark database covers 1413 data records from 32 datasets for 13 solutions. Evaluated datasets that are used in the parameterization of the relevant water-salt pair are also presented.

2. The consistent E-NRTL model is compared against the widely used original E-NRTL model. Results and parameters indicate that the consistent model better reconciles MIAC and VLE, especially the salting out effect of the co-solvent (alcohol) when it is highly diluted in water.

3. A consistency analysis is conducted within each solution. Impacts of the objective functions and water-salt parameters are discussed, facilitating the parameterization and data analysis. Recommended parameters are obtained based on the obtained benchmark database.

Considering that alcohol and monovalent strong salts represent the simplest components in mixed-solvent electrolyte solutions, we propose that the database be used as a benchmark for model development and evaluation, as thermodynamic property models are extended to mixed-solvent electrolyte solutions.

Nomenclature

A_φ	One third of the Debye-Huckel limiting slope
AD	Average deviation
E-NRTL	Electrolyte non-random two-liquid
G^{E}	Excess Gibbs energy
I_x	Ionic strength
k	Boltzmann constant
m	Molality
M	Molar mass
MD	Maximum deviation
MIAC	Mean ionic activity coefficient
n	Molar amount
N_{A}	Avogadro number

OF	Objective function
OF-M	OF = MIAC
OF-MV	OF = MIAC + VLE
OF-V	OF = VLE
p	Pressure
PDH	Pitzer-Debye-Huckel
Q_e	Elementary charge
r	Born radius
	Pauling radius
R	Universal gas constant
R	Recommended datasets
SLE	Solid-liquid equilibrium
T	Temperature
T	Tentative datasets
U	Uncertain datasets
VLE	Vapor-liquid equilibrium
w^0	Weight fraction on the salt-free basis
x	Molar fraction (in general or in the liquid phase)
x^0	Composition in the original unit
	Molar fraction on the salt-free basis
y	Molar fraction in the vapor phase

710	Z	Ionic charge
711	**Greek letters**	
712	α	Parameter in the NRTL term
713	γ	Activity coefficient
714	$\Delta g_{\mathrm{trans}}$	Molar Gibbs energy of transfer
715	$\Delta_{\mathrm{f}} g$	Standard Gibbs energy of formation
716	Δp	Vapor pressure depression
717	ε	Relative permittivity
718	ε_0	Dielectric constant in the vacuum
719	ν	Stoichiometric coefficient
720	ρ	Density
721	τ	Parameter in the NRTL term
722	**Subscript**	
723	$\pm$	Mean ionic
724	a	Anion
725	(a)	Reference state at infinite dilution in water
726	c	Cation
727	m	Molecule
728	s	Solvent mixture
729	(s)	Solid phase
730	w	Water

Superscript

*	Rational unsymmetrical
∞	Infinite dilution
m	Molality
c	Molarity
sat	Saturation state of pure solvent

Supporting Information

Supporting Information are provided for the following contents:

- Analytical expressions for $\left(\frac{\partial A_{\varphi}}{\partial n_i}\right)_{T,p,n_{j(j\neq i)}}$ and the other derivatives over n_i.
- Solvent activity coefficients of (water + methanol + KCl) and (water + ethanol + NaCl/KCl).
- Parameters for solvent component density and relative permittivity.
- Parameters of the consistent and original E-NRTL models for (water + methanol/ethanol + NaCl/KCl) with OF-M and OF-MV.
- Deviations of MIAC calculated with the E-NRTL model with OF-MV and parameters regressed in the region up to $x_{\mathrm{ion}} = 0.06$ and in the entire x_{ion} range.
- Average and maximum deviations of the e-NRTL model from the experimental datasets.
- Summary of accepted MIAC and VLE datasets for aqueous electrolyte solutions.
- Benchmark database files for the mixed-solvent electrolyte solutions and relevant aqueous electrolyte solutions.
- MIAC results for the mixed-solvent electrolyte solutions.

The information is available free of charge via the Internet at http://pubs.acs.org/.

Notes

The authors declare no competing financial interest.

Acknowledgement

The authors wish to thank the European Research Council (ERC) for funding of this research under European Union's Horizon 2020 research and innovation program (grant agreement No. 832460), ERC Advanced Grant project "New Paradigm in Electrolyte Thermodynamics".

Reference:

(1) Bui, M.; Adjiman, C. S.; Bardow, A.; Anthony, E. J.; Boston, A.; Brown, S.; Fennell, P. S.; Fuss, S.; Galindo, A.; Hackett, L. A.; Hallett, J. P.; Herzog, H. J.; Jackson, G.; Kemper, J.; Krevor, S.; Maitland, G. C.; Matuszewski, M.; Metcalfe, I. S.; Petit, C.; Puxty, G.; Reimer, J.; Reiner, D. M.; Rubin, E. S.; Scott, S. A.; Shah, N.; Smit, B.; Trusler, J. P. M.; Webley, P.; Wilcox, J.; Mac Dowell, N. Carbon Capture and Storage (CCS): The Way Forward. *Energy Environ. Sci.* **2018**, *11* (5), 1062–1176. https://doi.org/10.1039/c7ee02342a.

(2) Gholami, F.; Tomas, M.; Gholami, Z.; Vakili, M. Technologies for the Nitrogen Oxides Reduction from Flue Gas: A Review. *Sci. Total Environ.* **2020**, *714*, 136712. https://doi.org/10.1016/j.scitotenv.2020.136712.

(3) Darre, N. C.; Toor, G. S. Desalination of Water: A Review. *Curr. Pollut. Reports* **2018**, *4* (2), 104–111. https://doi.org/10.1007/s40726-018-0085-9.

(4) Løge, I. A.; Bentzon, J. R.; Klingaa, C. G.; Walther, J. H.; Anabaraonye, B. U.; Fosbøl, P. L. Scale Attachment and Detachment: The Role of Hydrodynamics and Surface Morphology. *Chem. Eng. J.* **2021**, *430* (P2), 132583. https://doi.org/10.1016/j.cej.2021.132583.

(5) Olasunkanmi, L. O. Corrosion: Favoured, yet Undesirable - Its Kinetics and Thermodynamics. In *Corrosion*; IntechOpen: London, 2021; pp 1–17.

(6) Yu, Z.; Wang, H.; Kong, X.; Huang, W.; Tsao, Y.; Mackanic, D. G.; Wang, K.; Wang, X.; Huang, W.; Choudhury, S.; Zheng, Y.; Amanchukwu, C. V.; Hung, S. T.; Ma, Y.; Lomeli, E. G.; Qin, J.; Cui, Y.; Bao, Z. Molecular Design for Electrolyte Solvents Enabling Energy-Dense and Long-Cycling Lithium Metal Batteries. *Nat. Energy* **2020**, *5* (7), 526–

533. https://doi.org/10.1038/s41560-020-0634-5.

(7) Molla, G. S.; Freitag, M. F.; Stocks, S. M.; Nielsen, K. T.; Sin, G. Solubility Prediction of Different Forms of Pharmaceuticals in Single and Mixed Solvents Using Symmetric Electrolyte Nonrandom Two-Liquid Segment Activity Coefficient Model. *Ind. Eng. Chem. Res.* **2019**, *58* (10), 4267–4276. https://doi.org/10.1021/acs.iecr.8b04268.

(8) Bazyleva, A.; Abildskov, J.; Anderko, A.; Baudouin, O.; Chernyak, Y.; de Hemptinne, J. C.; Diky, V.; Dohrn, R.; Elliott, J. R.; Jacquemin, J.; Jaubert, J. N.; Joback, K. G.; Kattner, U. R.; Kontogeorgis, G. M.; Loria, H.; Mathias, P. M.; O'Connell, J. P.; Schröer, W.; Smith, G. J.; Soto, A.; Wang, S.; Weir, R. D. Good Reporting Practice for Thermophysical and Thermochemical Property Measurements (IUPAC Technical Report). *Pure Appl. Chem.* **2021**, *93* (2), 253–272. https://doi.org/10.1515/pac-2020-0403.

(9) May, P. M.; Rowland, D. Correction to Thermodynamic Modeling of Aqueous Electrolyte Systems: Current Status (Journal of Chemical & Engineering Data (2017) 62:9 (2481-2495) DOI: 10.1021/Acs.Jced.6b01055). *J. Chem. Eng. Data* **2019**, *64* (7), 3212. https://doi.org/10.1021/acs.jced.9b00468.

(10) Kontogeorgis, G. M.; Dohrn, R.; Economou, I. G.; De Hemptinne, J. C.; Kate, A.; Kuitunen, S.; Mooijer, M.; Zilnik, L. F.; Vesovic, V. Industrial Requirements for Thermodynamic and Transport Properties: 2020. *Ind. Eng. Chem. Res.* **2021**, *60* (13), 4987–5013. https://doi.org/10.1021/acs.iecr.0c05356.

(11) Kontogeorgis, G. M.; Maribo-Mogensen, B.; Thomsen, K. The Debye-Hückel Theory and Its Importance in Modeling Electrolyte Solutions. *Fluid Phase Equilib.* **2018**, *462*, 130–152. https://doi.org/10.1016/j.fluid.2018.01.004.

(12) Simonin, J. P. On the "Born" Term Used in Thermodynamic Models for Electrolytes. *J. Chem. Phys.* **2019**, *150*, 244503. https://doi.org/10.1063/1.5096598.

(13) Thomsen, K. *Electrolyte Solutions: Thermodynamics, Crystallization, Separation Methods*; Technical University of Denmark: Kgs. Lyngby, 2009. https://doi.org/10.11581/dtu:00000073.

(14) Vaque Aura, S.; Roa Pinto, J. S.; Ferrando, N.; De Hemptinne, J. C.; Ten Kate, A.; Kuitunen, S.; Diamantonis, N.; Gerlach, T.; Heilig, M.; Becker, G.; Brehelin, M. Data Analysis for Electrolyte Systems: A Method Illustrated on Alkali Halides in Water. *J. Chem. Eng. Data* **2021**, *66* (8), 2976–2990. https://doi.org/10.1021/acs.jced.1c00105.

(15) Raatschen, W.; Harvey, A. H.; Prausnitz, J. M. Equation of State for Solutions of Electrolytes in Mixed Solvents. *Fluid Phase Equilib.* **1987**, *38* (1–2), 19–38. https://doi.org/10.1016/0378-3812(87)90002-1.

(16) Zuo, Y. X.; Fürst, W. Use of an Electrolyte Equation of State for the Calculation of Vapor-Liquid Equilibria and Mean Activity Coefficients in Mixed Solvent Electrolyte Systems. *Fluid Phase Equilib.* **1998**, *150* (151), 267–275. https://doi.org/10.1016/s0378-3812(98)00326-4.

(17) Simon, H. G.; Kistenmacher, H.; Prausnitz, J. M.; Vortmeyer, D. An Equation of State for Systems Containing Electrolytes and Nonelectrolytes. *Chem. Eng. Process.* **1991**, *29* (3), 139–146. https://doi.org/10.1016/0255-2701(91)85013-E.

(18) Zuo, J. Y.; Zhang, D.; Fürst, W. Predicting LLE in Mixed-Solvent Electrolyte Systems by an Electrolyte EOS. *AIChE J.* **2000**, *46* (11), 2318–2329. https://doi.org/10.1002/aic.690461122.

(19) Zuo, J. Y.; Zhang, D.; Fürst, W. Extension of the Electrolyte EOS of Furst and Renon to Mixed Solvent Electrolyte Systems. *Fluid Phase Equilib.* **2000**, *175* (1–2), 285–310. https://doi.org/10.1016/S0378-3812(00)00463-5.

(20) Held, C.; Reschke, T.; Mohammad, S.; Luza, A.; Sadowski, G. EPC-SAFT Revised. *Chem. Eng. Res. Des.* **2014**, *92* (12), 2884–2897. https://doi.org/10.1016/j.cherd.2014.05.017.

(21) Schreckenberg, J. M. A.; Dufal, S.; Haslam, A. J.; Adjiman, C. S.; Jackson, G.; Galindo, A. Modelling of the Thermodynamic and Solvation Properties of Electrolyte Solutions with the Statistical Associating Fluid Theory for Potentials of Variable Range. *Mol. Phys.* **2014**, *112* (17), 2339–2364. https://doi.org/10.1080/00268976.2014.910316.

(22) Maribo-Mogensen, B.; Thomsen, K.; Kontogeorgis, G. M. An Electrolyte CPA Equation of State for Mixed Solvent Electrolytes. *AIChE J.* **2015**, *61* (9), 2933–2950. https://doi.org/10.1002/aic.14829.

(23) Das, G.; dos Ramos, M. C.; McCabe, C. Predicting the Thermodynamic Properties of Experimental Mixed-Solvent Electrolyte Systems Using the SAFT-VR+DE Equation of State. *Fluid Phase Equilib.* **2018**, *460*, 105–118. https://doi.org/10.1016/j.fluid.2017.11.017.

(24) Ahmed, S.; Ferrando, N.; de Hemptinne, J. C.; Simonin, J. P.; Bernard, O.; Baudouin, O.

Modeling of Mixed-Solvent Electrolyte Systems. *Fluid Phase Equilib.* **2018**, *459*, 138–157. https://doi.org/10.1016/j.fluid.2017.12.002.

(25) Neau, E.; Nicolas, C.; Avaullée, L. Extension of the Group Contribution NRTL-PRA EoS for the Modeling of Mixtures Containing Light Gases and Alcohols with Water and Salts. *Fluid Phase Equilib.* **2018**, *458*, 194–210. https://doi.org/10.1016/j.fluid.2017.09.028.

(26) Mock, B.; Evans, L. B.; Chen, C. -C. Thermodynamic Representation of Phase Equilibria of Mixed-solvent Electrolyte Systems. *AIChE J.* **1986**, *32* (10), 1655–1664. https://doi.org/10.1002/aic.690321009.

(27) Chen, C. C.; Song, Y. Generalized Electrolyte-NRTL Model for Mixed-Solvent Electrolyte Systems. *AIChE J.* **2004**, *50* (8), 1928–1941. https://doi.org/10.1002/aic.10151.

(28) Macedo, E. A.; Skovborg, P.; Rasmussen, P. Calculation of Phase Equilibria for Solutions of Strong Electrolytes in Solvent-Water Mixtures. *Chem. Eng. Sci.* **1990**, *45* (4), 875–882. https://doi.org/10.1016/0009-2509(90)85009-3.

(29) Sander, B.; Fredenslund, A.; Rasmussen, P. Calculation of Vapour-Liquid Equilibria in Mixed Solvent/Salt Systems Using an Extended UNIQUAC Equation. *Chem. Eng. Sci.* **1986**, *41* (5), 1171–1183. https://doi.org/10.1016/0009-2509(86)87090-7.

(30) Zerres, H.; Prausnitz, J. M. Thermodynamics of Phase Equilibria in Aqueous-organic Systems with Salt. *AIChE J.* **1994**, *40* (4), 676–691. https://doi.org/10.1002/aic.690400411.

(31) Van Bochove, G. H.; Krooshof, G. J. P.; De Loos, T. W. Modelling of Liquid-Liquid Equilibria of Mixed Solvent Electrolyte Systems Using the Extended Electrolyte NRTL. *Fluid Phase Equilib.* **2000**, *171* (1–2), 45–58. https://doi.org/10.1016/S0378-3812(00)00347-2.

(32) Thomsen, K. Modeling Electrolyte Solutions with the Extended Universal Quasichemical (UNIQUAC) Model. *Pure Appl. Chem.* **2005**, *77* (3), 531–542. https://doi.org/10.1351/pac200577030531.

(33) Djamali, E.; Kan, A. T.; Tomson, M. B. A Priori Prediction of Thermodynamic Properties of Electrolytes in Mixed Aqueous-Organic Solvents to Extreme Temperatures. *J. Phys. Chem. B* **2012**, *116* (30), 9033–9042. https://doi.org/10.1021/jp301857m.

(34) Djamali, E.; Tomson, M. B.; Chapman, W. G. Thermodynamic Properties and Solubility of Sodium and Potassium Chloride in Ethane-1,2-Diol/Water Mixed Solvent Systems to

High Temperatures. *J. Chem. Eng. Data* **2017**, *62* (4), 1326–1334. https://doi.org/10.1021/acs.jced.6b00842.

(35) Hála, E. Vapor-Liquid Equilibria of Strong Electrolytes in Systems Containing Mixed Solvent. *Fluid Phase Equilib.* **1983**, *13*, 311–319. https://doi.org/https://doi.org/10.1016/0378-3812(83)80102-2.

(36) Iliuta, M. C.; Thomsen, K.; Rasmussen, P. Extended UNIQUAC Model for Correlation and Prediction of Vapour-Liquid-Solid Equilibria in Aqueous Salt Systems Containing Non-Electrolytes. Part A. Methanol-Water-Salt Systems. *Chem. Eng. Sci.* **2000**, *55* (14), 2673–2686. https://doi.org/10.1016/S0009-2509(99)00534-5.

(37) Thomsen, K.; Iliuta, M. C.; Rasmussen, P. Extended UNIQUAC Model for Correlation and Prediction of Vapor-Liquid-Liquid-Solid Equilibria in Aqueous Salt Systems Containing Non-Electrolytes. Part B. Alcohol (Ethanol, Propanols, Butanols)-Water-Salt Systems. *Chem. Eng. Sci.* **2004**, *59* (17), 3631–3647. https://doi.org/10.1016/j.ces.2004.05.024.

(38) Fosbøl, P. L.; Thomsen, K.; Stenby, E. H. Modeling of the Mixed Solvent Electrolyte System CO2-Na 2CO3-NaHCO3-Monoethylene Glycol-Water. *Ind. Eng. Chem. Res.* **2009**, *48* (9), 4565–4578. https://doi.org/10.1021/ie801168e.

(39) Guggenheim, E. A. L. The Specific Thermodynamic Properties of Aqueous Solutions of Strong Electrolytes. *London, Edinburgh, Dublin Philos. Mag. J. Sci.* **1935**, *19* (127), 588–643. https://doi.org/10.1080/14786443508561403.

(40) Christensen, C.; Sander, B.; Fredenslund, A.; Rasmussen, P. Towards the Extensionof UNIFAC to Mixtures with Electrolytes. *Fluid Phase Equilib.* **1983**, *13* (C), 297–309. https://doi.org/10.1016/0378-3812(83)80101-0.

(41) Pitzer, K. S. *Activity Coefficients in Electrolyte Solutions*, 2nd Editio.; CRC Press: Boca Raton Ann Arbor Boston London, 1991.

(42) Robinson, R. A.; Sinclair, D. A. The Activity Coefficients of the Alkali Chlorides and of Lithium Iodide in Aqueous Solution from Vapor Pressure Measurements. *J. Am. Chem. Soc.* **1934**, *56* (9), 1830–1835. https://doi.org/10.1021/ja01324a003.

(43) Robinson, R. A. The Osmotic and Activity Coefficient Data of Some Aqueous Salt Solutions from Vapor Pressure Measurements. *J. Am. Chem. Soc.* **1937**, *59* (1), 84–90. https://doi.org/10.1021/ja01280a019.

(44) Robinson, R. A. The Activity Coefficients of Some Alkali Halides at 25.°. *Trans. Faraday Soc.* **1939**, *35*, 1217–1220.

(45) Mussini, P. R.; Mussini, T.; Sala, B. Thermodynamics of the Cell {Li-Amalgam | LiX (m) | AgX | Ag} (X = Cl,Br) and Medium Effects upon LiX in (Acetonitrile + Water), (1,4-Dioxane + Water), and (Methanol + Water) Solvent Mixtures with Related Solvation Parameters. *J. Chem. Thermodyn.* **2000**, *32* (5), 597–616. https://doi.org/10.1006/jcht.1999.0622.

(46) Yang, R.; Demirgian, J.; Solsky, J. F.; Kikta, E. J.; Marinsky, J. A. Mean Molal Activity of Sodium Chloride, Potassium Chloride, and Cesium Chloride in Ethanol-Water Mixtures. *J. Phys. Chem.* **1979**, *83* (21), 2752–2761. https://doi.org/10.1021/j100484a013.

(47) Westhaus, U. DETHERM. DECHEMA e.V.: Frankfurt am Main 2019.

(48) Thomsen, K. Data Bank for Electrolyte Solutions. Technical University of Denmark: Kgs. Lyngby 2020.

(49) Advanced Tools for Optimization and Uncertainty Treatment. IFP Energies nouvelles: Rueil-Malmaison 2019.

(50) Span, R.; Wagner, W. A New Equation of State for Carbon Dioxide Covering the Fluid Region from the Triple-Point Temperature to 1100 K at Pressures up to 800 MPa. *J. Phys. Chem. Ref. Data* **1996**, *25* (6), 1509–1596. https://doi.org/10.1063/1.555991.

(51) Chen, C.; Britt, H. I.; Boston, J. F.; Evans, L. B. Local Composition Model for Excess Gibbs Energy of Electrolyte Systems. Part I: Single Solvent, Single Completely Dissociated Electrolyte Systems. *AIChE J.* **1982**, *28* (4), 588–596.

(52) Chen, C. -C; Evans, L. B. A Local Composition Model for the Excess Gibbs Energy of Aqueous Electrolyte Systems. *AIChE J.* **1986**, *32* (3), 444–454. https://doi.org/10.1002/aic.690320311.

(53) Chen, C. C. Toward Development of Activity Coefficient Models for Process and Product Design of Complex Chemical Systems. *Fluid Phase Equilib.* **2006**, *241* (1–2), 103–112. https://doi.org/10.1016/j.fluid.2006.01.006.

(54) Saravi, S. H.; Ravichandran, A.; Khare, R.; Chen, C. C. Bridging Two-Liquid Theory with Molecular Simulations for Electrolytes: An Investigation of Aqueous NaCl Solution. *AIChE J.* **2019**, *65* (4), 1315–1324. https://doi.org/10.1002/aic.16521.

(55) Renon, H.; Prausnitz, J. M. Local Compositions in Thermodynamic Excess Functions for

Liquid Mixtures. *AIChE J.* **1968**, *14* (1), 135–144. https://doi.org/10.1002/aic.690140124.

(56) Pitzer, K. S. Electrolytes. From Dilute Solutions to Fused Salts. *J. Am. Chem. Soc.* **1980**, *102* (9), 2902–2906. https://doi.org/10.1021/ja00529a006.

(57) Liu, Y.; Watanasiri, S. Representation of Liquid-Liquid Equilibrium of Mixed-Solvent Electrolyte Systems Using the Extended Electrolyte NRTL Model. *Fluid Phase Equilib.* **1996**, *116* (1–2), 193–200. https://doi.org/10.1016/0378-3812(95)02887-0.

(58) Robinson, R. A.; Stokes, R. H. *Electrolyte Solutions, 2nd Edition*; Dover Publications: Mineola, 2002.

(59) Rashin, A. A.; Honig, B. Reevaluation of the Born Model of Ion Hydration. *J. Phys. Chem.* **1985**, *89* (26), 5588–5593. https://doi.org/10.1021/j100272a006.

(60) Chang, C. K.; Lin, S. T. Extended Pitzer-Debye-Hückel Model for Long-Range Interactions in Ionic Liquids. *J. Chem. Eng. Data* **2020**, *65* (3), 1019–1027. https://doi.org/10.1021/acs.jced.9b00368.

(61) Song, Y.; Chen, C. C. Symmetric Electrolyte Nonrandom Two-Liquid Activity Coefficient Model. *Ind. Eng. Chem. Res.* **2009**, *48* (16), 7788–7797. https://doi.org/10.1021/ie9004578.

(62) Tsanas, C.; de Hemptinne, J.-C.; Mougin, P. Calculation of Phase and Chemical Equilibrium for Multiple Ion-Containing Phases Including Stability Analysis. *Chem. Eng. Sci.* **2021**, 117174. https://doi.org/10.1016/j.ces.2021.117174.

(63) Mohr, P. J.; Newell, D. B.; Taylor, B. N. CODATA Recommended Values of the Fundamental Physical Constants: 2014. *J. Phys. Chem. Ref. Data* **2016**, *45*, 043102. https://doi.org/10.1063/1.4954402.

(64) Wilding, W. V.; Rowley, R. L.; Oscarson, J. L. DIPPR® Project 801 Evaluated Process Design Data. *Fluid Phase Equilib.* **1998**, *150* (151), 413–420. https://doi.org/10.1016/s0378-3812(98)00341-0.

(65) Raspo, I.; Neau, E. An Empirical Correlation for the Relative Permittivity of Liquids in a Wide Temperature Range: Application to the Modeling of Electrolyte Systems with a GE/EoS Approach. *Fluid Phase Equilib.* **2020**, *506*, 112371. https://doi.org/10.1016/j.fluid.2019.112371.

(66) Xu, Y.; Li, S.; Zhai, Q.; Jiang, Y.; Hu, M. Investigation on the Thermodynamic Properties of KCl/CsCl + NaCl + CH3OH + H2O Quaternary Systems at 298.15K. *J. Ind. Eng.*

Chem. **2014**, *20* (4), 2159–2165. https://doi.org/10.1016/j.jiec.2013.09.046.

(67) Basili, A.; Mussini, P. R.; Mussini, T.; Rondinini, S. Thermodynamics of the Cell: {NaxHg1-X|NaCl(m)|AgCl|Ag} in (Methanol + Water) Solvent Mixtures. *J. Chem. Thermodyn.* **1996**, *28* (8), 923–933. https://doi.org/10.1006/jcht.1996.0081.

(68) Yang, S. O.; Lee, C. S. Vapor-Liquid Equilibria of Water + Methanol in the Presence of Mixed Salts. *J. Chem. Eng. Data* **1998**, *43* (4), 558–561. https://doi.org/10.1021/je970286w.

(69) Basili, A.; Mussini, P. R.; Mussini, T.; Rondinini, S.; Vertova, A. Thermodynamics of the Amalgam Cell: {MexHg1-X|MeCl(m)| AgCl| Ag} (with Me = K, Rb) in (Methanol+water) Solvent Mixtures. *Berichte der Bunsengesellschaft für Phys. Chemie* **1997**, *101* (5), 842–846. https://doi.org/https://doi.org/10.1002/bbpc.19971010510.

(70) Esteso, M. A.; Gonzalez-Diaz, O. M.; Hernandez-Luis, F. F.; Fernandez-Merida, L. Activity Coefficients for NaCl in Ethanol-Water Mixtures at 25 C. *J. Solution Chem.* **1989**, *18* (3), 277–288.

(71) Mamontov, M. N.; Konstantinova, N. M.; Uspenskaya, I. A. Water-Ethanol-Sodium Chloride System: The Main Sources of Uncertainties in Thermodynamic Properties Determined by Potentiometry. *Fluid Phase Equilib.* **2016**, *412*, 62–70. https://doi.org/10.1016/j.fluid.2015.12.012.

(72) Mussini, P. R.; Mussini, T.; Perelli, A.; Rondinini, S.; Vertova, A. Thermodynamics of the Cell: {MexHg1−x|MeCl(m)|AgCl|Ag} (Me = Na,K,Cs) in (Ethanol + Water) Solvent Mixtures. *J. Chem. Thermodyn.* **1995**, *27* (3), 245–251. https://doi.org/https://doi.org/10.1006/jcht.1995.0022.

(73) Yan, Y.; Chen, C. C. Thermodynamic Representation of the NaCl+Na2SO4+H2O System with Electrolyte NRTL Model. *Fluid Phase Equilib.* **2011**, *306* (2), 149–161. https://doi.org/10.1016/j.fluid.2011.03.023.

(74) Harned, H. S. A Rule for the Calculation of the Activity Coefficients of Salts in Organic Solvent-Water Mixtures. *J. Phys. Chem.* **1962**, *66* (4), 589–591. https://doi.org/10.1021/j100810a004.

(75) Basili, A.; Mussini, P. R.; Mussini, T.; Rondinini, S.; Sala, B.; Vertova, A. Transference Numbers of Alkali Chlorides and Characterization of Salt Bridges for Use in Methanol+water Mixed Solvents. *J. Chem. Eng. Data* **1999**, *44* (5), 1002–1008.

https://doi.org/10.1021/je9900979.
(76) Hu, M.; Tang, J.; Li, S.; Xia, S.; Jiang, Y. Activity Coefficients of Lithium Chloride in ROH/Water Mixed Solvent (R = Me, Et) Using the Electromotive Force Method at 298.15 K. *J. Chem. Eng. Data* **2008**, *53* (2), 508–512. https://doi.org/10.1021/je700614h.
(77) Broul, M.; Hlavatý, K.; Linek, J. Liquid-Vapour Equilibrium in Systems of Electrolytic Components. V. The System CH3OH-H2O-LiCl at 60 °C. *Collect. Czechoslov. Chem. Commun.* **1969**, *34* (11), 3428–3435.
(78) Yao, J.; Yan, W. D.; Xu, Y. J.; Han, S. J. Activity Coefficients for NaCl in MeOH + H2O by Electromotive Force Measurements at 308.15 K and 318.15 K. *J. Chem. Eng. Data* **1999**, *44* (3), 497–500. https://doi.org/10.1021/je970288g.
(79) Hernández-Hernández, F.; Pérez-Villaseñor, F.; Hernández-Ruiz, V.; Iglesias-Silva, G. A. Activity Coefficients of NaCl in H2O + MeOH + EtOH by Electromotive Force at 298.15 K. *J. Chem. Eng. Data* **2007**, *52* (3), 959–964. https://doi.org/10.1021/je600549h.
(80) Yao, J.; Li, H.; Han, S. Vapor-Liquid Equilibrium Data for Methanol-Water-NaCl at 45 °C. *Fluid Phase Equilib.* **1999**, *162* (1–2), 253–260. https://doi.org/10.1016/S0378-3812(99)00204-6.
(81) Johnson, A. I.; Furter, W. F. Salt Effect in Vapor-Liquid Equilibrium. *Can. J. Chem. Eng.* **1960**, *38* (3), 78–87.
(82) Zhang, J.; Gao, S.-Y.; Xia, S.-P.; Yao, Y. Study of Thermodynamic Properties of Quaternary Mixture RbCl + Rb2SO 4 + CH 3OH + H2O by EMF Measurement at 298.15 K. *Fluid Phase Equilib.* **2004**, *226* (1–2), 307–312. https://doi.org/10.1016/j.fluid.2004.10.010.
(83) Hu, M.; Cui, R.; Li, S.; Jiang, Y.; Xia, S. P. Determination of Activity Coefficients for Cesium Chloride in Methanol-Water and Ethanol-Water Mixed Solvents by Electromotive Force Measurements at 298.15 K. *J. Chem. Eng. Data* **2007**, *52* (2), 357–362. https://doi.org/10.1021/je060278s.
(84) Cui, R. F.; Hu, M. C.; Jin, L. H.; Li, S. N.; Jiang, Y. C.; Xia, S. P. Activity Coefficients of Rubidium Chloride and Cesium Chloride in Methanol-Water Mixtures and a Comparative Study of Pitzer and Pitzer-Simonson-Clegg Models (298.15 K). *Fluid Phase Equilib.* **2007**, *251* (2), 137–144. https://doi.org/10.1016/j.fluid.2006.11.016.
(85) Falciola, L.; Longoni, G.; Mussini, P. R.; Mussini, T. Thermodynamics of the Amalgam

Cells {Cs-Amalgam|CsX (m)|AgX|Ag} (X = Cl, Br, I) and Primary Medium Effects in (Methanol + Water), (Acetonitrile + Water), and (1,4-Dioxane + Water) Solvent Mixtures. *J. Chem. Thermodyn.* **2006**, *38* (6), 788–798. https://doi.org/10.1016/j.jct.2005.08.014.

(86) Hernández-Luis, F.; Vázquez, M. V; Esteso, M. A. Activity Coefficients for NaF in Methanol-Water and Ethanol-Water Mixtures at 25 °C. *J. Mol. Liq.* **2003**, *108* (1), 283–301. https://doi.org/https://doi.org/10.1016/S0167-7322(03)00187-9.

(87) BOONE, J. E.; ROUSSEAU, R. W.; SCHOENBORN, E. M. The Correlation of Vapor-Liquid Equilibrium Data for Salt-Containing Systems. In *Thermodynamic Behavior of Electrolytes in Mixed Solvents*; Advances in Chemistry; AMERICAN CHEMICAL SOCIETY, 1976; Vol. 155, pp 36–52. https://doi.org/doi:10.1021/ba-1976-0155.ch004.

(88) Han, S.; Pan, H. Thermodynamics of the Sodium Bromide-Methanol-Water and Sodium Bromide-Ethanol-Water Two Ternary Systems by the Measurements of Electromotive Force at 298.15K. *Fluid Phase Equilib.* **1993**, *83* (C), 261–270. https://doi.org/10.1016/0378-3812(93)87029-Z.

(89) Hernández-Luis, F.; Galleguillos, H. R.; Graber, T. A.; Taboada, M. E. Activity Coefficients of LiCl in Ethanol - Water Mixtures at 298.15 K. *Ind. Eng. Chem. Res.* **2008**, *47* (6), 2056–2062. https://doi.org/10.1021/ie070704i.

(90) Shaw, R.; Butler, J. A. V. The Behavior of Electrolytes in Mixed Solvents. Part II. - The Effect of Lithium Chloride on the Activities of Water and Alcohol in Mixed Solvents. *Proc. R. Soc. London. Ser. A - Math. Phys. Sci.* **1930**, *129*, 519–536.

(91) Meyer, T.; Poika, H. M.; Gmehling, J. Low-Pressure Isobarle Vapor-Liquid Equilibria of Ethanol/Water Mixtures Containing Electrolytes. *J. Chem. Eng. Data* **1991**, *36* (3), 340–342. https://doi.org/10.1021/je00003a023.

(92) Sun, R. Molecular Thermodynamics of Salt Effect in Vapor-Liquid Equilibrium - Calculation of Isobaric VLE Salt Effect Parameters for Ethanol-Water-1-1 Type Electrolyte Systems. *CIESC J.* **1996**, *47* (4), 401-409 (in Chinese).

(93) González-Díaz, O. M.; Fernández-Mérida, L.; Hernández-Luis, F.; Esteso, M. A. Activity Coefficients for NaBr in Ethanol-Water Mixtures at 25 °C. *J. Solution Chem.* **1995**, *24* (6), 551–563. https://doi.org/10.1007/BF00973206.

(94) BURNS, J. A.; FURTER, W. F. Effects of Salts Having Large Organic Ions on Vapor-Liquid Equilibrium. In *Advances in Chemistry, Thermodynamic Behavior of Electrolytes*

in Mixed Solvents; Advances in Chemistry; AMERICAN CHEMICAL SOCIETY, 1976; Vol. 155, pp 99–127. https://doi.org/doi:10.1021/ba-1976-0155.ch008.

(95) Du, Y.; Tang, J.; Li, S.; Zhai, Q.; Jiang, Y.; Hu, M. Activity Coefficients for CsBr + MeOH/EtOH + H2O Ternary Systems Using Potentiometric Measurements at 298.15 K. *J. Chem. Eng. Data* **2012**, *57* (9), 2603–2609. https://doi.org/10.1021/je300671y.

(96) Yamamoto, H.; Terano, T.; Yanagisawa, M.; Tokunaga, J.; Nishi, Y.; Tokunaga, J. Salt Effect of CACL2, NH4i and NAI on Vapor-Liquid Equilibrium of Ethanol + Water System at 298.15 K. *Can. J. Chem. Eng.* **1995**, *73* (5), 779–783. https://doi.org/https://doi.org/10.1002/cjce.5450730522.

(97) Burns, J. A.; Furter, W. F. Salt Effect in Vapor-Liquid Equilibrium At Fixed Liquid Composition. *Adv. Chem. Ser.* **1979**, No. 177, 11–26. https://doi.org/10.1021/ba-1979-0177.ch002.

(98) Akerlof, G. Activity Coefficients of Sodium, Potassium and Lithium Chlorides and Hydrochloric Acid at Infinite Dilution in Water-Methyl Alcohol Mixtures. *J. Am. Chem. Soc.* **1930**, *52*, 2353–2368.

(99) Yan, W.; Xu, Y.; Han, S. Activity Coefficients of Sodium Chloride in Methanol-Water Mixed Solvents at 298.15 K. *Acta Chim. Sin.* **1994**, *52* (10), 937-946 (in Chinese).

(100) Deyhimi, F.; Abedi, M. NaCl + CH 3OH + H 2O Mixture: Investigation Using the Pitzer and the Modified Pitzer Approaches to Describe the Binary and Ternary Ion-Nonelectrolyte Interactions. *J. Chem. Eng. Data* **2012**, *57* (2), 324–329. https://doi.org/10.1021/je201084a.

(101) Kozłowski, Z.; Bald, A.; Gregorowicz, J. Thermodynamic Studies of NaCl Solutions in Water + Methanol Mixtures by Means of a Galvanic Cell Containing a Glass Sodium Electrode. *J. Electroanal. Chem.* **1990**, *288* (1–2), 75–82. https://doi.org/10.1016/0022-0728(90)80026-3.

(102) Jödecke, M.; Kamps, Á. P. S.; Maurer, G. Experimental Investigation of the Influence of NaCl on the Vapor-Liquid Equilibrium of CH3OH + H2O. *J. Chem. Eng. Data* **2005**, *50* (1), 138–141. https://doi.org/10.1021/je049783k.

(103) Sun, R. Calculation of Salting Effect on Vapor-Liquid Equilibrium in Water-Nonelectrolyte Systems. *Chem. Eng.* **1995**, *23* (1), 13–17, 30 (in Chinese).

(104) Abedi, M.; Shendi, M. A.; Karimzadeh, Z.; Salamat-Ahangari, R.; Deyhimi, F. The

Ternary and Quaternary Electrolyte Systems: Activity Coefficient of NaCl Measured and Modeled for NaCl + C2H5OH + H2O and NaCl + KCl + C2H5OH + H2O Systems. *Fluid Phase Equilib.* **2016**, *423*, 138–145. https://doi.org/10.1016/j.fluid.2016.04.023.

(105) Chen, W.; Zhang, W. Vapor-Liquid Equilibria for Alcohol-Water-KI/NaAc Systems. *J. Chem. Eng. Chinese Univ.* **2003**, *17* (2), 123-127 (in Chinese).